Thesis for the degree of Doctor of Philosophy

Planar Heterostructure Barrier Varactor Diodes for Millimetre Wave Applications

Jan Stake

Submitted to the School of Electrical and Computer Engineering,
Chalmers University of Technology,
in partial fulfilment of the requirements for the degree of
Doctor of Philosophy

CHALMERS

Department of Microelectronics ED
Chalmers University of Technology
Göteborg, Sweden 1999

Planar Heterostructure Barrier Varactor Diodes for
Millimetre Wave Applications

© JAN STAKE
ISBN 91-7197-774-0

Doktorsavhandlingar vid Chalmers Tekniska Högskola
Ny serie 1481
ISSN 0346-718X

Technical Report No. 360
School of Electrical Engineering and Computer Engineering
Chalmers University of Technology
SE-412 96 Göteborg
Sweden
Telephone + 46 (0)31-7721000

Cover:
An eight barrier (4x2) planar HBV (CTH-NU2003J)

Printed by Bibliotekets Reproservice
Chalmers University of Technology
Göteborg, February 1999

Abstract

This thesis deals with fabrication, characterisation and modelling of the Heterostructure Barrier Varactor (HBV) diode and its use in frequency multiplier applications. Different aspects of material structures and frequency multipliers are described. The aim of the work presented is to develop design methods and processes to fabricate state-of-the-art planar HBVs and multipliers in the millimetre and submillimetre wave length region.

Results from AlGaAs HBV frequency tripler measurements are presented. Simulations and cooled measurements show that excessive conduction current due to self-heating degrades the multiplier efficiency. A new design of planar GaAs-based HBVs with reduced thermal resistance and series resistance have been fabricated. A state-of-the-art performance of 4,8 % efficiency and an output power of 4 mW at 246 GHz was achieved.

A novel fabrication process where HBV diodes are fabricated on a copper substrate is proposed. This reduces thermal resistance and parasitic resistance without degrading the electrical characteristics.

A 141 GHz quasi-optical HBV tripler is presented. A peak flange-to-flange efficiency of 8 % and an output power of 11,5 mW was achieved.

Different III-V material systems for HBVs have been tested. The results of lattice matched and pseudomorphic GaAs/AlGaAs, InGaAs/InAlAs, InAs/AlSb and phosphide containing materials for HBVs are presented. The state-of-the-art material for millimetre and submillimetre wave HBVs is the $In_{0,53}GaAs/In_{0,52}AlAs$ system with a thin AlAs layer (30 Å) in the middle of the barrier.

Both simple analytical models and a self-consistent Poisson/Schrödinger approach are used to predict and optimise HBV diodes. Finally, a simple quick-design method for calculation of optimum embedding impedances, optimum conversion efficiency and pump power for HBV triplers are presented.

Key Words

Heterostructure Barrier Varactor (HBV), millimetre and submillimetre wave power source, varactor diode, frequency multiplier, III-V semiconductor.

List of publications

The thesis is based on the following papers:

A. J. Stake, L. Dillner, S. H. Jones, C. M. Mann, J. Thornton, J. R. Jones, W. L. Bishop, and E. L. Kollberg, "Effects of Self-Heating on Planar Heterostructure Barrier Varactor Diodes," *IEEE Trans. Electron Devices*, vol. 45, no. 11, pp. 2298-2303, 1998.

B. J. Stake, C. M. Mann, L. Dillner, S. H. Jones, S. Hollung, H. Mohamed, B. Alderman and E. L. Kollberg, "Improved Diode Geometry for Planar Heterostructure Barrier Varactors," presented at *Tenth International Symposium on Space Terahertz Technology*, Charlottesville, 1999.

C. L. Dillner, J. Stake, and E. L. Kollberg, "Heterostructure Barrier Varactors on Copper Substrate," *Electronics. Lett.*, vol. 35, no. 4, 1999.

D. J. Stake, S. H. Jones, L. Dillner, and S. Hollung, "Heterostructure Barrier Varactor Design," *manuscript*, 1999.

E. L. Dillner, J. Stake, and E. L. Kollberg, "Analysis of Symmetric Varactor Frequency Multipliers," *Microwave Opt. Technol. Lett.*, vol. 15, pp. 26-29, 1997.

F. Y. Fu, J. Stake, L. Dillner, M. Willander, and E. L. Kollberg, "AlGaAs/GaAs and InAlAs/InGaAs Heterostructure Barrier Varactors," *J. Appl. Phys.*, vol. 82, pp. 5568-5572, 1997.

G. S. Hollung, J. Stake, L. Dillner, and E. L. Kollberg, "A 141-GHz Quasi-Optical HBV Diode Frequency Tripler," presented at *Tenth International Symposium on Space Terahertz Technology*, Charlottesville, 1999.

H. J. Stake and H. Grönqvist, "An On-Wafer Method for C-V Characterisation of Heterostructure Diodes," *Microwave and Opt. Technol. Lett*., vol. 9, pp. 63-66, 1995.

I. J. Stake, L. Dillner and M. Ingvarson, "Fabrication and Characterisation of Heterostructure Barrier Varactor Diodes," Report No. 29 (revised), Department of Microwave Technology, Chalmers University of Technology, 1996.

The following publications are not included due to an overlap in contents or a content which goes beyond the scope of this thesis:

R1. L. Kollberg, J. Stake and L. Dillner, "Heterostructure barrier varactors at submillimetre waves," *Phil. Trans. R. Soc. Lond. A*, vol 354, pp. 2383-2398, 1996.

R2. L. Dillner and J. Stake, "Analysis of Heterostructure Barrier Varactor Frequency Multipliers," Report No. 27, Department of Microwave Technology, Chalmers University of Technology, 1996.

R3. K. Fobelets, C. Van Hoof, J. Genoe, J. Stake, L. Lundgren and G. Borghs, "High frequency capacitance of bipolar resonant tunneling diodes," *J. Appl. Phys.*, vol. 79, pp. 905-910, 1996.

R4. J. Stake, S. H. Jones, J. R. Jones, and L. Dillner, "Analysis of Carrier Transport in a Heterostructure Barrier Varactor Diode Tripler," presented at *1997 International Semiconductor Device Research Symposium*, Charlottesville, 1997.

R5. L. Dillner, J. Stake, and E. L. Kollberg, "Modeling of the Heterostructure Barrier Varactor Diode," presented at *1997 International Semiconductor Device Research Symposium*, Charlottesville, 1997.

R6. Y. Fu, L. Dillner, J. Stake, M. Willander, and E. L. Kollberg, "Capacitance Analysis for AlGaAs/GaAs and InAlAs/InGaAs Heterostructure Barrier Varactor Diodes," *J. Appl. Phys.*, vol. 83, pp. 1457-1462, 1998.

R7. J. Stake, L. Dillner, S. H. Jones, E. L. Kollberg, and C. M. Mann, "Design of 100-900 GHz AlGaAs/GaAs Planar Heterostructure Barrier Varactor Frequency Triplers," presented at *Ninth International Symposium on Space Terahertz Technology,* Pasadena, 1998.

R8. S. Mahiey, C. M. Mann, J. Stake, L. Dillner, S. H. Jones, and J. Thornton, "A Broadband Frequency Tripler for SIS Receivers," presented at *Ninth International Symposium on Space Terahertz Technology*, Pasadena, 1998.

R9. E. L. Kollberg, L. Dillner, and J. Stake, "Heterostructure Barrier Varactor Multipliers," presented at *ESA Workshop on Millimetre Wave Technology and Applications*, Espoo, Finland, 1998.

R10. L. Dillner, J. Stake, S. Hollung, and E. Kollberg, "Heterostructure Barrier Varactors on Copper Substrate for Generation of Millimeter- and Submillimeter-Waves," presented at *Tenth International Symposium on Space Terahertz Technology*, Charlottesville, 1999.

R11. S. Hollung, J. Stake, L. Dillner, and E. Kollberg, "A 141-GHz Integrated Quasi-Optical Slot Antenna Tripler," submitted to the *IEEE AP-S International Symposium and USNC/URSI National Radio Science Meeting*, Orlando, 1999.

R12. Y. Fu, J. Stake, L. Dillner, M. Willander, and E. L. Kollberg, "Carrier Conduction in a Heterostructure Barrier Varactor Induced by an AC Bias," *submitted to the J. Appl. Phys*, 1999.

Table of contents

List of Acronyms

A	Device area
C	Differential capacitance
$E_{g,dir}$	Direct energy gap
$E_{g,ind}$	Indirect energy gap
f_c	Cut-off frequency
f_p	Pump frequency
HBV	Heterostructure Barrier Varactor
HF	High Frequency
HFET	Heterostructure Field Effect Transistor
IF	Intermediate Frequency
L_D	Debye length
L_n	Conversion loss
LO	Local Oscillator
MBE	Molecular Beam Epitaxy
MMIC	Monolithic Microwave Integrated Circuit
MOCVD	Metal Organic Chemical Vapour Deposition
n	Order of multiplication
N	Number of stacked barriers
RF, rf	Radio Frequency
RT	Room Temperature
S	Differential elastance (=1/C)
SI	Semi-Insulating
V	External bias
V_a	Voltage over the accumulated layer
V_d	Voltage over the depleted layer
w	Length of the depleted region
δ	Skin depth

1. Introduction

Radio astronomy and military applications have for a long time been the driving force for the development of technology for sensitive receivers in the millimetre- and submillimetre wavelength range. The technology to build these sensitive heterodyne receivers involves development of low noise mixers and generation of sufficient local oscillator power. In recent years there has been an intensive development towards civilian applications (links, radars etc.) in the millimetre wave region (30 - 300 GHz). A major issue for new applications is that not only the technical aspects are important but also the cost. However, submillimetre wave (0,3 - 3 THz) technology still seems to be a field for basic research applications (e.g. radio astronomy). The main reason is that the existing technology is too expensive at these frequencies.

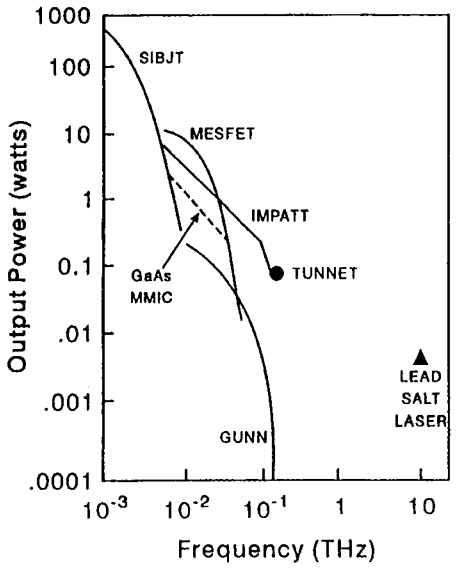

Figure 1: Conventional (fundamental) solid state sources.

When going to higher frequencies, a general problem is that the available output power becomes smaller. Existing direct generators such as Gunn or IMPATT oscillators are out of question as solid state submillimetre wave sources [Yngvesson 1991]. The shrinking dimensions (volume) and the decreasing DC to RF power efficiency (typically 5% at 100 GHz) creates heat problems. In Figure 1 the output power from some conventional solid state sources are shown. The output power drops rapidly with the frequency. Today, to reach the terahertz frequency range with a solid state source, the solution is to use a frequency multiplier.

Varactor multipliers [Penfield 1962; Faber 1995] rather than varistor multipliers are preferred at submillimetre wave frequencies because they exhibit a much higher conversion efficiency. They are the only all-solid-state technology capable of generating the required power with the necessary spectral purity, stability and low noise, to drive the mixer in a receiver. A reverse biased Schottky diode can be used as a varactor diode. When the Schottky diode is pumped, its non-linear capacitance generates harmonics. The external circuit impedance matches the diode and filters the desired harmonic. For a tripler, it is also necessary to maximise the current at the second harmonic with an idler circuit. When the Schottky diode is forward biased, the multiplication is mainly due to the non-linear I-V characteristic (i.e. varistor diode). For a survey of Schottky diode technology and its use in multipliers and mixers, see reference [Crowe 1995].

The Heterostructure Barrier Varactor (HBV) diode, first proposed by Kollberg *et al.* [1989], is a promising varactor device for millimetre and submillimetre wave power generation. The HBV is a symmetric device and will therefore only generate odd harmonics. This implies that there is no need for DC-bias and no need for an idler circuit for a frequency tripler. Consequently, an HBV tripler is easier to design and can be matched over a larger bandwidth [Mahiey 1998]. Especially in sensitive SIS receivers, a reduced number of generated harmonics (spuriouses) improves the overall system performance compared to the use of a Schottky multiplier source. However, the design, material growth and fabrica-

tion of the semiconductor devices are more difficult than Schottky diode structures used in similar applications. Competing new varactors with symmetric C-V characteristics are the Schottky/2-DEG/Schottky diode [Peatman 1992] and the back to back Barrier-N-layer-N^+ diode [Lieneweg 1992].

When first introduced, the HBV design was focused on mesa diodes for whisker contacting. This work was followed by fabrication of planar geometry HBVs operating from 230 – 260 GHz [Jones 1997; Stake 1999b]. Most recently, excellent planar HBV tripler results demonstrating 12% and 9 mW at 247 GHz have been reported by Mélique *et al.* [1999]. The planar diode is more robust and allows circuit integration. Furthermore, at 300 GHz the waveguide is typically 100 µm high and 800 µm wide. Hence, considerable machining and assembly skills are required to fabricate such a device and cost is a limiting factor. In the near future, advances within micromachining of waveguides [Crowe 1997; Mann 1997; Lubecke 1998] and novel planar device fabrication techniques will reduce production cost and hence make inexpensive integrated submillimetre wave RF-front-ends feasible.

2. The Heterostructure Barrier Varactor Diode

The HBV is one of many new high speed devices based on the advances in epitaxial techniques such as Molecular Beam Epitaxy (MBE) [Cho 1983] and Metal Organic Chemical Vapour Deposition (MOCVD) [Dupuis 1984]. This breakthrough in material science means that thickness, doping and composition of individual epitaxial layers can be tailored for a certain application. A limitation is that the lattice constant must be kept constant through the structure (Figure 2). However, thin strained (pseudomorphic) layers with a slightly different lattice constant can be grown to optimise the device performance even further.

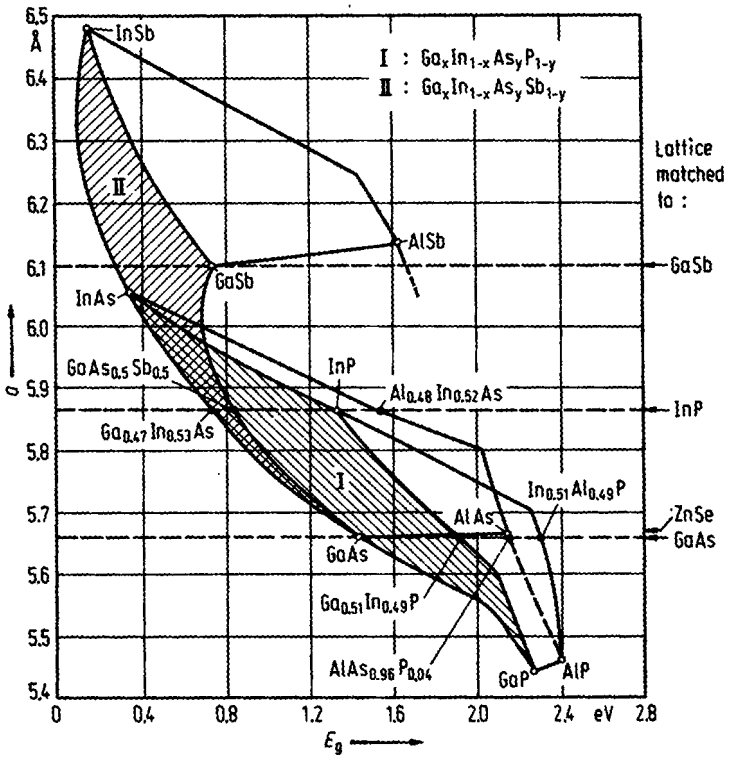

Figure 2: Lattice constant vs. energy gap (RT) for various III-V compounds and their alloys [Madelung 1991].

Low band gap material systems are especially useful for high frequency applications. It is easy to form good ohmic contacts and the mobility is high. The disadvantage is the low breakdown voltage which is a limitation for high power applications. For the HBV there is a trade-off between breakdown voltage and losses (mobility). The HBV has only been realised in the III-V material system.

The HBV is fabricated using standard III-V processing techniques [Stake 1996]. This involves optical lithography, electron beam lithography (EBL) for mask generation, wet/dry etching techniques and metallisation techniques.

2.1 Basic principles

The HBV diode is an unipolar device and consists of a symmetric layer structure. An undoped high band gap material (barrier) is sandwiched between two moderately n-doped low band gap materials. The barrier prevents electron transport through the structure. Hence, the barrier should be undoped (no carriers), high and thick enough to minimise thermionic emission and tunnelling of carriers. When the diode is biased a depleted region builds up (Figure 3) causing a non-linear CV curve.

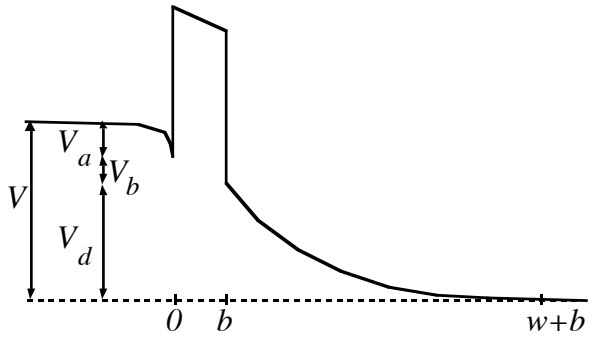

Figure 3: Conduction band for a biased single barrier. The length of the depleted region is w.

Contrary to the Schottky diode, where the barrier is formed at the interface bet-ween a metallic contact and a semiconductor, the HBV uses a heterojunction as blocking element. A heterojunction, i.e. two adjacent epitaxial semiconductor layers with different band gaps, exhibits band discontinuities both in the valence and in the conduction band. The main advantage of using heterostructures for varactor devices, is that several barriers can be epitaxially stacked. Since the distance between the barriers (>1000 Å) is large compared to the de Broglie-wavelength of the electron, it is possible to understand the stacked barrier structure as a series connection of *N* individual barriers. A generic layer structure of an HBV is shown in Table I.

Table I: *Generic layer structure of an HBV. For N epitaxially stacked barriers, the layer sequence 2-5 is repeated N times.*

Layer		Thickness [Å]	Doping level [cm^{-3}]
7	Contact	*~ 3000*	n^{++}
6	Modulation	*l = 3000*	$N_d \sim 10^{17}$
5	Spacer	*s = 50*	*undoped*
4	Barrier	*b = 110*	*undoped*
3	Spacer	*s = 50*	*undoped*
2	Modulation	*l = 3000*	$N_d \sim 10^{17}$
1	Buffer	-	n^{++}
0	Substrate		n^{++} *or SI*

2.1.1 Equivalent circuit

The Uhlir [1958] model of a pure varactor diode has only two elements (Figure 4): a non-linear (differential) elastance, *S(V)=1/C(V),* and a constant parasitic series resistance, R_s. The model is very useful in analytical and numerical analysis of harmonic frequency multipliers [Tang 1966; Krishnamurthi 1993; Dillner 1997a].

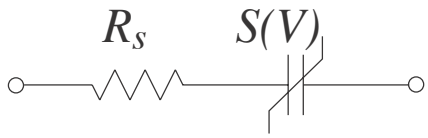

Figure 4: Equivalent circuit of a pure varactor diode (i.e. no conduction current).

The performance of a non ideal pure varactor device is associated with the dynamic cut-off frequency

$$f_c = \frac{S_{\max} - S_{\min}}{2\pi R_s} \tag{1}$$

where S_{max} and S_{min} are the maximum and minimum elastance, respectively, during a pump cycle. However, a more realistic non-linear quasistatic model of the HBV diode is shown in Figure 5. The series resistance is frequency dependent due to the skin effect and voltage dependent through the extension of the depleted region. The inductance, *L,* models the diode connection (airbridge, bonding wire etc.).

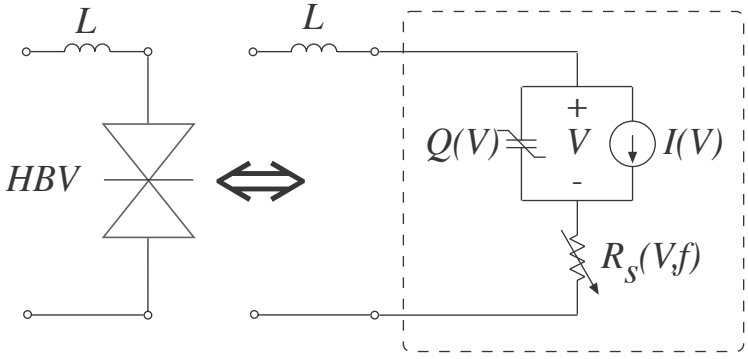

Figure 5: Quasistatic equivalent circuit model of the HBV diode.

The non-linear equivalent circuit in Figure 5 can be extracted from measured reflection coefficients using a Vector Network Analyser (VNA) at different biases [Stake 1995]. The large signal equivalent circuit is thus replaced with a bias dependent small signal equivalent circuit. To ensure linear operation, it is important to keep the RF power low without violating the signal to noise ratio. The non-linear current source (I-V) and the non-linear capacitance (C-V) are linearised at the bias point as:

$$G(V) = \frac{\partial I(V)}{\partial V}$$
$$C(V) = \frac{1}{S(V)} = \frac{\partial Q(V)}{\partial V} \tag{2}$$

The extracted parameters can be used in a large signal frequency multiplier simulation up to the submillimetre wavelength range, where inertial effects become important [Jones 1994b; Lipsey 1997] and as long as the effect of current saturation is negligible [Kollberg 1992]. The above effects can be analysed in more detail using an integrated hydrodynamic device/harmonic balance simulator [Jones 1995b], see Section 3.3 , or with the quasistatic HBV model reported by Adamski *et al.* [1998].

2.1.2 The HBV capacitance

The parallel plate capacitor model, where the plate separation should be replaced with the sum of the barrier thickness (Table I), b, the spacer layer thickness, s, and the length of the depleted region, w, is normally an adequate description of the (differential) capacitance. The depletion length is bias dependent and the layer structure is symmetric, therefore the elastance is an even function of applied voltage given by

$$S = \frac{1}{C} = \frac{N}{A}\left(\frac{b}{\varepsilon_b} + \frac{s}{\varepsilon_d} + \frac{w}{\varepsilon_d}\right)$$
$$w = \sqrt{\frac{2\varepsilon_d |V_d|}{qN_d}} \tag{3}$$

where V_d is the voltage across the depleted region, N_d is the doping concentration in the modulation layer, b is the barrier thickness, s is the undoped spacer layer thickness, A is the device area, ε_b and ε_d are the dielectric constants in the barrier material and modulation layers, respectively. The maximum capacitance or the minimum elastance, S_{min}, occurs at zero bias. However, due to screening effects, the minimum elastance, S_{min}, must include the extrinsic Debye length, L_D, as:

$$S_{\min} = \frac{1}{C_{\max}} = \frac{N}{A}\left(\frac{b}{\varepsilon_b} + \frac{2s}{\varepsilon_d} + \frac{2L_D}{\varepsilon_d}\right)$$
$$L_D \equiv \sqrt{\frac{\varepsilon_d kT}{q^2 N_d}} \tag{4}$$

To achieve a high C_{max}/C_{min} ratio, the screening length can be minimised with a sheet doping, N_s, at the spacer/depletion layer interface. The minimum capacitance, C_{min}, is normally obtained for punch through condition, i.e. $w = l$, or when the breakdown voltage, V_{max}, is reached. When the barrier thickness is of the same order as the penetration length of an

electron wave, the maximum capacitance, C_{max}, is only weakly dependent on the barrier thickness [Fu 1998] and equation 4 is not valid. For a high C_{max} value, the electron barrier must be thin and high enough to keep the wave penetration length short.

The theory for a surface space-charge region in thermal equilibrium [e.g. Sze 1981b; Mönch 1993] can be used to accurately calculate the C-V characteristic for a homogeneously doped HBV (Figure 6). The effect of a sheet doping at the spacer/depletion layer interface on the capacitance modulation ratio is also shown in Figure 6.

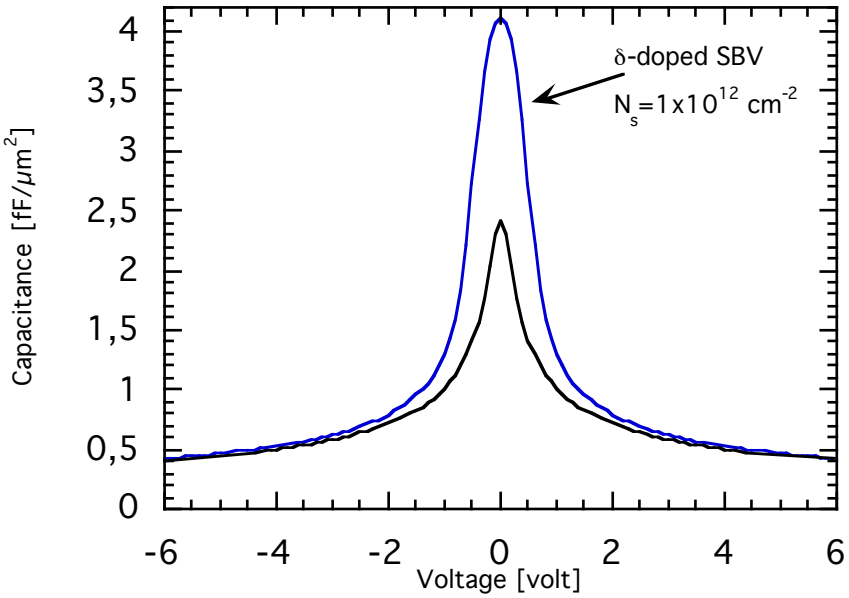

Figure 6: *Calculated room temperature C-V characteristic for a single barrier $In_{.53}GaAs/In_{.52}AlAs$ HBV. Input data for the calculation are shown in Table I. The influence of a sheet-doping ($N_s=10^{12}$ cm^{-2}) at the spacer/depletion layer interface is also shown.*

From the above theory, an accurate quasi-empirical expression for the C-V characteristic of homogenously doped HBVs has been derived [Dillner 1997b]. The voltage across the non-linear capacitor is expressed as a function of its charge as

$$V(Q) = N\left(\frac{bQ}{\varepsilon_b A} + 2\frac{sQ}{\varepsilon_d A} + Sign(Q)\left(\frac{Q^2}{2qN_d\varepsilon_d A^2} + \frac{4kT}{q}\left(1 - e^{-\frac{|Q|}{2L_D AqN_d}}\right)\right)\right) \qquad (5)$$

where T is the device temperature, q is the elementary charge, and Q is the charge stored in the HBV. The C-V characteristic can be calculated from the quasi-empirical expression (5) as dQ/dV and is shown together with the measured C-V curve in Figure 7. The C-V characteristic was measured with an LCR-meter (HP4285) at 18 MHz.

In modulating the capacitance at submillimetre wave frequencies, the electron depletion edge cannot move faster than the saturated electron velocity, and thus the actual capacitance modulation ratio is limited by velocity saturation effects [Ruch 1970].

2.1.3 Current vs. voltage

The I-V characteristic, which is anti-symmetrical, is mainly determined by thermionic emission over the barrier and/or tunnelling through the barrier. The dominating mechanism depends on temperature, barrier height and barrier thickness.

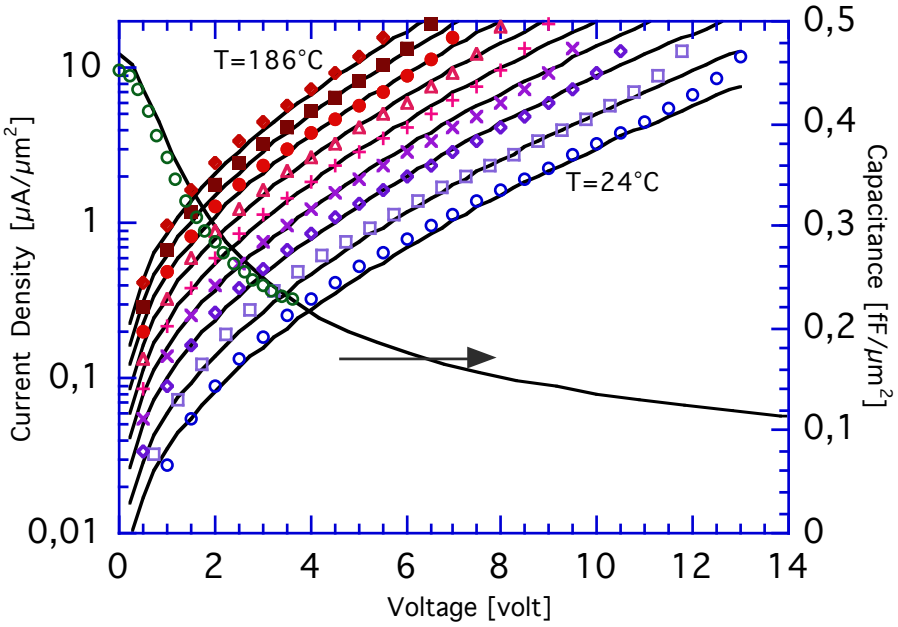

Figure 7: *Measured and modeled conduction current and C-V characteristic for the 4-barrier HBV diode (UVA-NRL-1174), see Table III. The C-V curve was measured at room temperature. The conduction current was measured on a hot-plate at different temperatures (RT-186°C). Due to symmetry, only positive voltages are shown in this figure. The parameters* a = 170 A/(m^2K^2), $E_o = 4.2\times10^6$ V/m, *and* ϕ_b = 0.17 eV *were used for the I-V model, equation 6.*

The tunnelling current is mainly direct for low voltages when $V_b < \Delta E_c$ *[eV]* (Figure 8a). For $V_b > \Delta E_c$ *[eV]* carriers are injected into the conduction band of the barrier (Figure 8b).

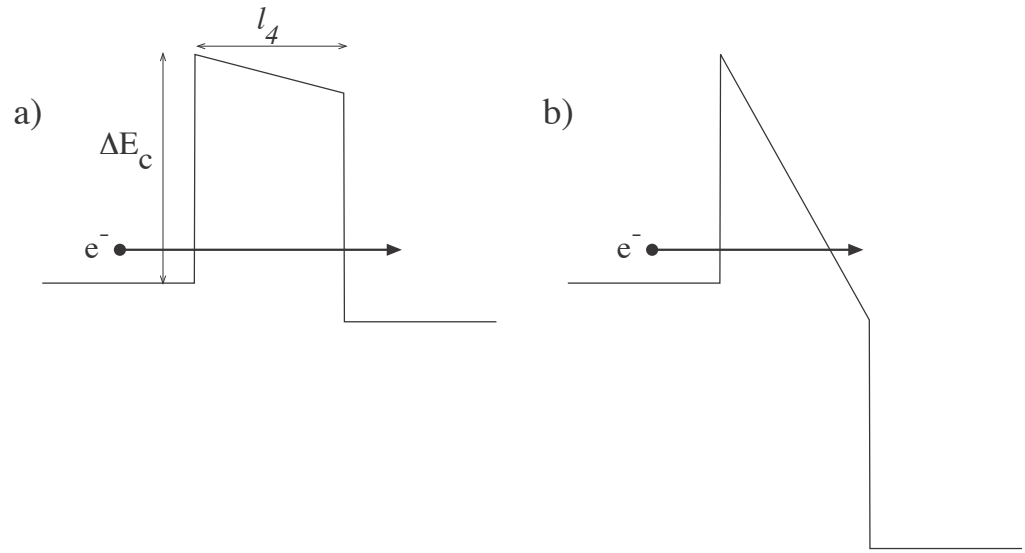

Figure 8: *Direct tunnelling (a) and Fowler-Nordheim injection (b).*

Several numerical techniques have recently been developed to calculate the I-V characteristic given a general barrier structure and adjacent modulation layers [Hjelmgren 1991; Fu 1997]. The dependence of the barrier thickness on the current density for a fixed external bias and the influence of a thin AlAs layer in the middle of the barrier is shown in Figure 9. If the barrier is thick, the effect of the AlAs layer is negligible.

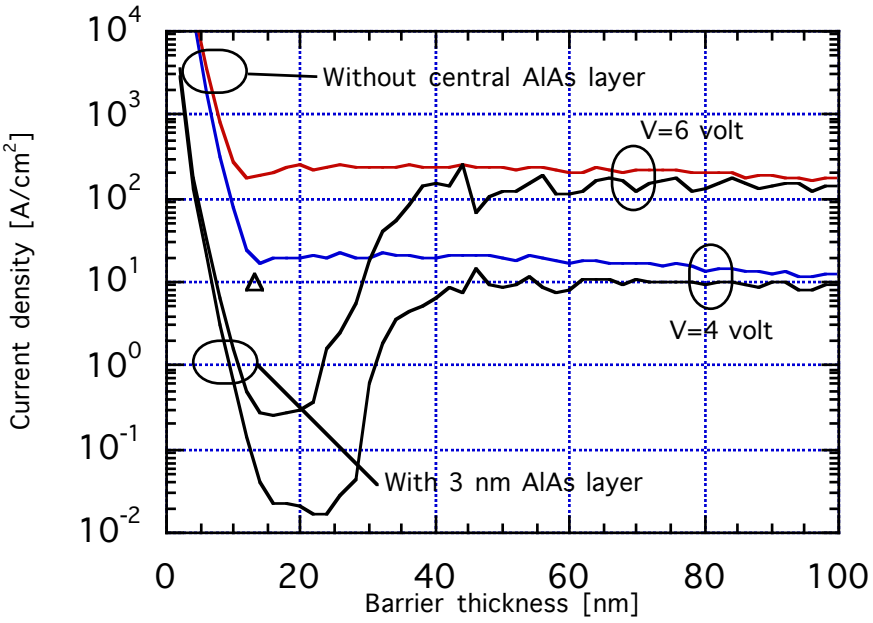

Figure 9: *Self-consistent Poisson/Schrödinger calculation of the current density (RT) for a single barrier HBV in the $In_{0,53}GaAs/In_{0,52}AlAs$ system as a function of the barrier thickness. The influence of a thin (3 nm) central AlAs layer for two different external biases is shown. The optimum total barrier thickness is approximately 20 nm. Δ from Lheurette et al. [1996].*

However, solving the Poisson equation and the Schrödinger equation self-consistently for an AC-bias is not yet feasible [Fu 1999]. Hence, quasi-static models of the I-V characteristic is the only choice for calculating the RF-performance of an HBV. If thermionic emission is dominant, the following empirical model describes the conduction current over the heterojunction barrier as a function of bias and temperature as

$$I(E_b) = A \cdot a \cdot T^2 Sinh\left(\frac{E_b}{E_o}\right) e^{-\frac{\phi_b}{kT}} \tag{6}$$

where E_b is the electric field in the barrier and can be implicitly calculated from (5) and Gauß's law, $Q=\varepsilon_b E_b$, or if electron screening effects are neglected as:

$$E_b(V) = Sign(V) \cdot qN_d \frac{b\varepsilon_d + 2s\varepsilon_b}{\varepsilon_b^2}\left(\sqrt{1 + \frac{2\varepsilon_d \varepsilon_b^2 |V|}{NqN_d\left(b\varepsilon_d + 2s\varepsilon_b\right)^2}} - 1\right). \tag{7}$$

The parameters a, E_o, and ϕ_b in (6) must be extracted from I-V measurements. An excellent fit with measured *I-V* characteristic for the HBV material UVA-NRL-1174 is shown in Figure 7. As a comparison, a current versus voltage characteristic of an HBV made in the InAs/AlSb system is shown in Figure 10. The conduction current is very low compared to the GaAs HBV shown in Figure 7.

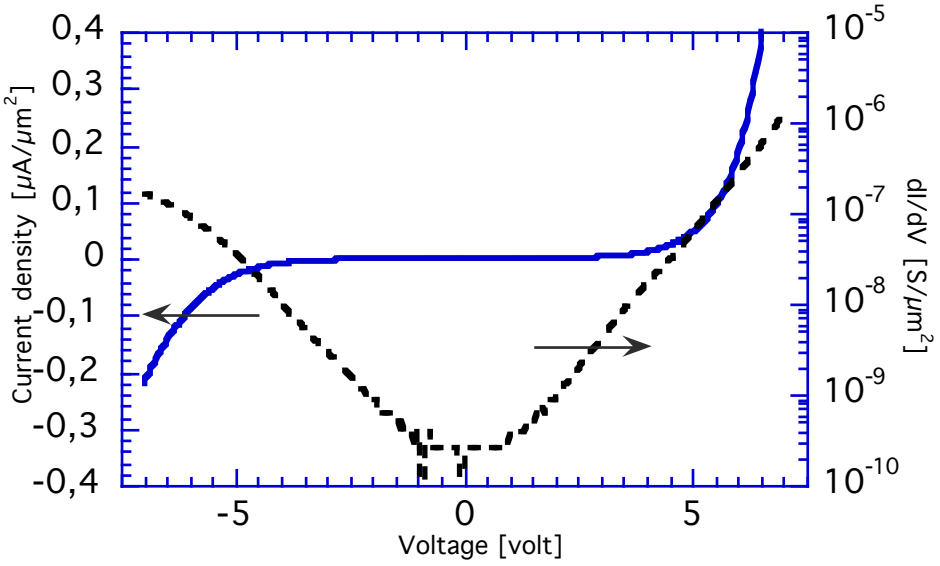

Figure 10: *I-V measurement performed at room temperature on device No. G1674 [layer structure: Stake 1996]. The device was fabricated in the InAs/AlAsSb material system.*

2.1.4 The series resistance

The multiplier performance critically depends on the losses within the device, R_s. Unfortunately, R_s is very difficult to measure. It is even hard to determine R_s from DC-measurements, given the large junction resistance over the normal operating range of the device. The use of RF-extraction methods of the series resistance is limited due to the high Q-value of the diode. From a sensitivity analysis [Stake 1996], the accuracy in the series resistance from an S-parameter measurement can never be better than:

$$\frac{\Delta R_s}{R_s} = \frac{\left(R_s + Z_o\right)^2}{2R_s Z_o}\Delta\Gamma \tag{8}$$

where Z_o is the characteristic impedance and $\Delta\Gamma$ is the measurement error of the reflection coefficient, Γ. Ohmic contact resistance can be measured using appropriate test structures [e.g. Williams 1990] and should be included on the wafer for in-process monitoring (PCM).

The series resistance is the sum of the resistance of the undepleted active layers (No. 2 and 6), the spreading resistance, the contact/buffer layer (No. 1 and 7) resistance and the ohmic contact resistance, R_c. The spreading resistance is caused by the material near the anode and at higher frequencies the skin effect becomes significant [Dickens 1967], and thus the shape of the geometry of the chip becomes important. Since the losses determine the multiplier performance, it is important to choose a suitable diode geometry and optimise the ohmic contact formation process for a low series resistance.

At terahertz frequencies, other effects are important. Plasma resonances in the epilayers and effects related to electron velocity saturation degrades the performance. The latter, sometimes referred to as current saturation, can be modelled as an effective series resistance which increases rapidly with pump power [Kollberg 1992].

2.2 Materials and epitaxial layer structure

A generic HBV layer structure is shown in Table I. The substrate is either highly doped or semi-insulating (SI), depending on how the device is intended to be mounted. The contact layers (No. 1 and 7) should be optimised for low losses. Therefore, the buffer layer (No. 1) must be relatively thick (δ~3 μm) and highly doped for planar HBVs, see Figure 11. It has been suggested to dope the barrier in order to improve the C_{max}/C_{min} value [Nilsen 1992]. However, this improvement will be at the expense of a much larger leakage current. The barrier itself can consist of different layers to further improve the blocking characteristic. The spacer prevents diffusion of dopants into the barrier layer and increases the effective barrier height.

The thickness of the barrier layer will not influence the cut-off frequency but it has some influence on the optimum embedding impedances. Hence, the thickness is chosen to be

thick enough to avoid tunnelling of carriers. Some semiconductors and their relevant electrical and thermal properties for HBVs are shown in Table II.

Table II: Bulk properties of some semiconductors at room temperature [Madelung 1991].

Material	$E_{g,dir}/E_{g,ind}$ [eV]	μ [cm^2/Vs]	v_{max} [cm/s]	$\varepsilon_r(0)$	κ [W/cmK]
Si	3,37/1,12	1450	8×10^6	11,9	1,5
Ge	0,81/0,66	3900	6×10^6	16,2	0,6
6H-SiC	4,4/2,86	900	-	9,66	5
AlP	3,62/2,45	60	-	9,80	0,9
AlAs	3,03/2,15	290	-	10,06	-
AlSb	2,21/1,62	200	-	12,04	0,3
GaN	3,44/-	440	-	10,4	1,4
GaP	2,78/2,27	160	-	11,11	1
GaAs	1,42/1,81	9200	$1,8\times10^7$	12,85	0,46
GaSb	0,75/0,80	3750	-	15,69	0,4
InP	1,34/1,80	5900	$2,5\times10^7$	12,56	0,7
InAs	0,35/1,21	33000	$3,6\times10^7$	15,15	0,3
InSb	0,18/0,62	70000	5×10^7	16,80	-

The transport mechanism at breakdown is not known. However, impact ionisation in the depleted layer seems to contribute to the increase of current for low band-gap materials, see Figure 10. For GaAs impact ionisation starts to occur when a hot electron *($E > 1.5E_g$)* relaxes and creates a new electron-hole pair after entering the depletion region. A rough estimate of the breakdown voltage can be made with the universal breakdown voltage expression for the abrupt PN junction [Sze 1981b]

$$V_{d,\max} = 60\left(\frac{E_g}{1,1}\right)^{3/2}\left(\frac{N_d}{10^{16}}\right)^{-3/4} \tag{9}$$

where E_g is the room temperature band gap energy in eV and N_d is the doping concentration in cm^{-3}. $V_{d,max}$ refers to the maximum allowed voltage across the depleted layer (Figure 3).

Several III-V semiconductor material systems have been employed for HBVs. The material quality is often low and the knowledge of processing is limited. Since it is hard to keep the growth conditions constant, the reproducibility is often low. The consequence is that the development of novel HBV structures so far have been slowed down.

The best choices for HBVs are the lattice matched $In_{0,53}Ga_{0,47}As/In_{0,52}Al_{0,48}As$ system grown on InP substrate and the lattice matched GaAs/AlGaAs system grown on GaAs substrate. High cut-off frequencies are achieved in both systems. However, the GaAs/AlGaAs system is well characterised and relatively easy to process which increases the probability of reproducible results. The $In_{0,53}GaAs/In_{0,52}AlAs$ system exhibit a higher electron barrier and is therefore advantageous from a leakage current point of view.

In general, it is recommendable to incorporate a thin very high band gap layer (e.g. AlAs) in the middle of the barrier. The leakage current is reduced due to lower thermionic emission and a reduction of Fowler-Nordheim injection. Furthermore, an InAs top contact layer improves the ohmic contact.

In the future, research on wide band gap semiconductors (e.g. InGaN) could provide solutions for very high power HBVs, a combination of a II-VI barrier for low leakage current and III-V modulation layer for high mobility and peak velocity, and the use of silicon wafer bonding techniques to fabricate $Si/SiO_2/Si$ HBVs. Today, narrow band gap semiconductors from the III-V groups (e.g. $In_xGa_{1-x}As$) seem to be the most suitable for submillimetre wave applications.

2.2.1 Lattice matched GaAs/AlGaAs on GaAs

The first HBV was fabricated in the AlGaAs system [Kollberg 1989]. The disadvantage of this system is the low barrier height, which leads to an excessive leakage current. The reported multiplier performance is therefore quite low [Rydberg 1990]. The first planar HBVs were fabricated with a homogenous $Al_{0,7}GaAs$ barrier, see Table III, and a non-optimal diode geometry with high thermal resistance (~2 K/mW) [Jones 1997]. Consequently, self heating of these HBVs [Stake 1998], results in an enhanced conduction current as the temperature increases, and hence, a reduced multiplier efficiency.

Table III: UVA-NRL-1174 Layer Structure

Material	Doping [cm^{-3}]	Thickness [Å]
InAs	1×10^{19}	100
$In_{1-0}GaAs$	1×10^{19}	400
GaAs	1×10^{19}	3000
GaAs	8×10^{16}	2500
GaAs	Undoped	35
$Al_{0,7}GaAs$	Undoped	200
GaAs	Undoped	35
GaAs	8×10^{16}	5000
GaAs	Undoped	35
$Al_{0,7}GaAs$	Undoped	200
GaAs	Undoped	35
GaAs	8×10^{16}	2500
GaAs	1×10^{19}	40000
GaAs	SI	-

The effective barrier height is low (~180 meV) even for Al-rich barriers. The reason is that the $Al_xGa_{1-x}As$ material is an indirect band gap semiconductor for $x > 0{,}41$, and for barriers with a thickness > 40 Å, a parasitic $\Gamma \rightarrow X$ transfer current dominates over the direct $\Gamma \rightarrow \Gamma$ current [Batey 1986; Landheer 1989].

By placing a thin AlAs layer in the centre of an $Al_{0,4}Ga_{0,6}As$ barrier one can increase the effective barrier height (372 meV) [Krishnamurthi 1994]. However, aluminium has an extremely high affinity for atmospheric oxygen. In combination with no good passivating dielectric, this means that surface effects can destroy the device performance, particularly for submicron devices where the total surface area becomes comparable with the active

device junction area. The barrier height can be further improved by using low band gap spacer layers In_xGaAs [Jones 1994a; Duez 1998]. The reported DC-performance is excellent [Duez 1998] and the C_{max}/C_{min} ratio is increased due to electron confinement closer to the barriers.

2.2.2 Lattice matched and pseudomorphic InGaAs/InAlAs on InP

Lattice matched $In_{0,53}Ga_{0,47}As/In_{0,52}Al_{0,48}As$ grown on semi-insulating Fe doped InP substrates is a very good material system for HBVs. The state-of-the-art HBV material with a very low leakage current (J_{max} = 10 A/cm^2 @ 6 V bias per barrier) has been fabricated in this material system [Lheurette 1996]. The $\Gamma \rightarrow \Gamma$ barrier energy is approximately 480 meV, which can be further optimised with a pseudomorphic (30 Å) AlAs layer in the centre of the barrier. Consequently, these devices are less sensitive to heating and excellent tripler performance has been reported [Rahal 1995; Mélique 1998a; Mélique 1998b]. The C_{max}/C_{min} ratio can be improved with a planar doping and a quantum well adjacent to the barrier [Lheurette 1998]. However, the escaping and trapping mechanism of such quantum wells at high frequencies has not yet been fully investigated.

2.2.3 Pseudomorphic InGaAs/InGaP on InP

The InGaP material has a very low surface recombination velocity of 10^3 cm/s compared to the AlGaAs value of 10^6 cm/s. The absence of the highly reactive aluminium means that the fabrication is not so critical. The high etch selectivity between InGaAs and InGaP provides accurate control of the mesa etch.

2.2.4 Pseudomorphic InAs/AlSb on InAs

The AlSb/InAs is a type II heterostructure, which means that it exhibits a negative valence band discontinuity. The idea of using this material system for HBVs is to combine the high intrinsic mobility (33000 cm^2/Vs) and the high drift velocity ($\approx 4 \times 10^7$ cm/s) in InAs with the high electron barrier (1,35 eV) in this system. For the HBV structure, an excellent barrier is formed in the conduction band, which has been experimentally verified (Figure 10), but holes can accumulate in the shallow quantum well in the valence band of the barrier. This quantum well should be broken with a thin layer of pure AlAs.

The experimental low frequency C-V characteristic is poor. This may be associated with interface electron traps [Tuttle 1990; Kroemer 1992], which may affect the low frequency C-V characteristic. It is difficult to process these materials, since the AlSb layer oxidises very quickly and therefore needs protection. The low breakdown voltage and more complicated processing techniques make the InAs/AlSb material system less useful for HBV fabrication.

2.2.5 Metamorphic InGaAs/InAlAs on GaAs

The lattice mismatched growth of InGaAs/InAlAs heterostructures on GaAs substrates have attracted much attention for different applications [Inoue 1991; Mishima 1995]. Not only because of the possibility to optimise the In content for a certain application but also that GaAs rather than InP substrates are preferable from a manufacturing point of view.

The availability of larger wafers, better robustness, and lower cost are some of the important advantages.

The technique to avoid dislocations is to grow a linearly or step graded InGaAs or InAlAs buffer. The thickness of the buffer layer is typically 1 µm. The quality of MBE grown graded buffer layers is good and even MMICs have been reported [Rohdin 1995].

2.3 Fabrication of HBVs

Until now, most of the utilised diodes in the submillimetre wave region are of the whisker contacted type. A honeycomb array of several thousand circular diodes on a highly doped substrate is fabricated and one of these anodes is contacted with an electrolytically sharpened whisker wire. The second contact consists of a large area backside ohmic contact. The main disadvantage of the whiskered devices is the inherent limitation for implementation of filter structures.

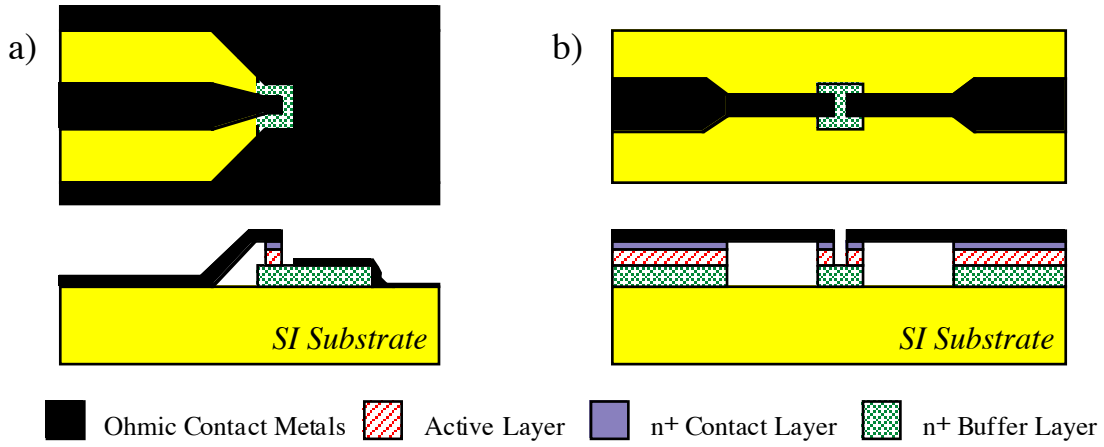

Figure 11: *Top and cross-sectional views of two different planar HBV topologies. The planar technique (a) is useful for coplanar on-wafer probing (MMICs). The surface channel diode technology (b), developed at the University of Virginia [Jones 1997].*

Planar diode structures are appropriate for integration and more robust than the whiskered diode. However, the electrical performance at submillimetre wave frequencies is still better for the whisker contacted diode. The reason is the high airbridge (finger) capacitance, the pad to pad capacitance and the higher parasitic resistance. Different concepts have been proposed to avoid these problems. The surface channel approach (Figure 11), introduced by Bishop *et al.* [1987], is one way to minimise parasitic capacitances. Another technology is the quasi-vertical approach [Simon 1993] which exhibits low losses and is more suitable for monolithic integration. With a selective via-hole etching, the mesa is located on the backside ohmic contact, giving a purely vertical current flow. However, the quasi-vertical approach is a rather complex technology due to the combination of critical back side (via-hole) and top side processing. We have chosen to fabricate the planar diodes shown in Figure 11b.

The main steps for fabricating planar HBV diodes are:

1. Cleaning
2. Ohmic contact formation

3. Device isolation
4. Passivation (if required)
5. Planarisation
6. Air bridge formation
7. Dicing into individual chips
8. Lapping of the substrate

Several of the process steps, especially step 1-3, have a strong influence on HBV device performance. Hence, it is important to maintain a high level of cleanliness and to continuously develop the fabrication procedure. Details of the device processing at Chalmers can be found in [Rorsman 1992; Nilsen 1994; Stake 1996] and general III-V semiconductor processing in [Williams 1990; Katz 1992].

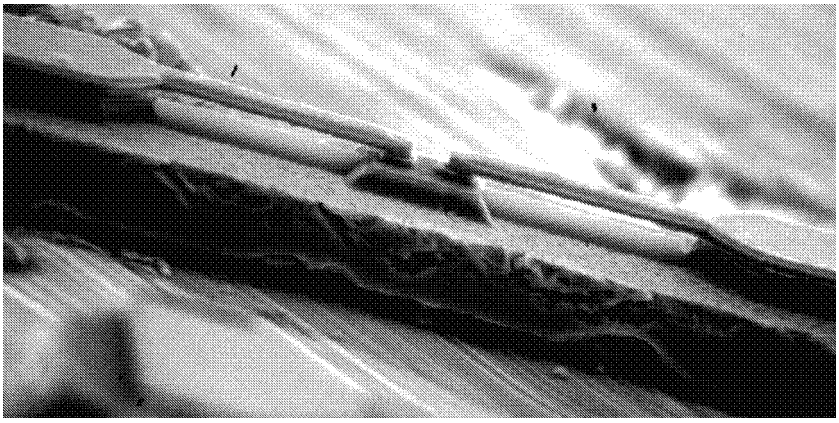

Figure 12: Planar four-barrier HBV (57 μm^2) from the CTH-NU2003J batch. The substrate is lapped to a thickness of ~20 μm.

The design of a high power planar HBV geometry must consider the effects of self-heating [Stake 1998]. As the device temperature increases, the mobility decreases, the maximum electron velocity decreases [Ruch 1970], and thermionic emission increases and hence the multiplier performance is degraded. The thermal resistance can be reduced by using shorter, thicker and wider airbridges and thicker substrates. However, there is certainly a trade-off between thermal and electromagnetic properties of a planar design. Recently, a novel InP-HBV whisker fabrication process has been proposed [Dillner 1999]. The InP substrate is removed through an epitaxial lift-off technique and replaced with a Cu-heat sink. The Cu-substrate should reduce the series resistance as well.

2.4 HBV diode optimisation

A simple design strategy for HBVs, similar to the work by Crove *et al.* [1996] for Schottky diodes, is described in this section. The cut-off frequency should be maximised for high efficiency. However, for terahertz operation the current saturation effect, $i_{sat} = qN_dAv_{sat}$, must be taken into account [Kollberg 1992]. The design goal is to maximise the cut-off frequency with the current saturation effect as an optimisation constraint. Since the series resistance depends on the diode geometry and the number of stacked barriers, the input power and the diode geometry affects the optimal layer structure.

For a given diode geometry, the design procedure is as follows:

1. Estimate the number of barriers that are needed to handle the input power [see Stake 1999a].

2. Calculate the epitaxial layer thickness, l_{max}, to be consistent with the saturated electron velocity

$$l_{\max} = \frac{v_{sat}}{4kf_p} \tag{10}$$

where $k \approx 2$, f_p is the pump frequency, and v_{sat} is the saturated electron velocity [Louhi 1995]. The factor, k, is the ratio between the saturated electron velocity, v_{sat}, and the average electron velocity during one-half of the pump cycle. Assuming a sinusoidal current waveform, the factor k is equal to $\pi/2$. From Harmonic Balance analysis of HBV triplers, k is typically between 1,5 and 2, hence, use $k=2$.

3. The modulation layer thickness should be large enough to accommodate the full depletion layer thickness under the maximum voltage during multiplier operation. A thicker layer adds series resistance while a thinner reduces the elastance modulation ratio. The diode should not undergo avalanche breakdown before the depletion layer is fully depleted. Using the empirical expression (9) for the breakdown voltage in Equation 3 yields:

$$l = w_{\max} = \sqrt{\frac{2\varepsilon_d V_{d,\max}}{qN_d}} \tag{11}$$

4. To obtain high multiplier efficiency, the dynamic cut-off frequency should be maximised. Hence, find the maximum value of Equation 1 combined with Equations 3, 4, 9, and 11 by varying the doping concentration of the modulation layer. For the optimisation and a given diode geometry, a proper model of the series resistance including dopant dependent mobility data [Sze 1981a] is needed. Ensure that the modulation layer thickness, l, does not become larger than the maximum value given by Equation 10.

5. The barrier thickness should be chosen to minimise the leakage current. The thickness of the barrier, b, can be estimated if the onset of Fowler-Nordheim injection (i.e. $V_b = \Delta E_c$ [eV]) is at the maximum allowed voltage, $V_{d,max}$. Increasing the barrier thickness will have a minor effect on the current density, since the electric field, E, is constant within the barrier. Hence, as a guideline the barrier thickness is given by

$$b = \frac{\Delta E_c}{E_b(V_d)} = \frac{\varepsilon_b}{\varepsilon_d} \frac{\Delta E_c q L_D}{\sqrt{2}kT\sqrt{e^{-\frac{qV_{d,\max}}{kT}} + \frac{qV_{d,\max}}{kT} - 1}} \tag{12}$$

where ΔE_c is in eV. Using Equation 9 for the breakdown voltage, the required barrier thickness as a function of the doping concentration can be calculated.

In the pseudomorphic case, with a thin high band gap layer in the middle of the barrier, the optimum total barrier thickness is approximately given by $2V_b=\Delta E_c\ [eV]$. For a more accurate result, self consistent Poisson/Schrödinger calculations should be employed.

6. Choose the diode area, using a large signal simulation, so the available input power can be absorbed without device breakdown. If the optimal embedding impedances are not feasible, redesign the HBV from step 3 with a different number of barriers.

3. Frequency multiplier circuits

Frequency multipliers are extensively used to provide LO-power to sensitive submillimetre wavelength receivers [e.g. Oswald 1998]. Solid-state multipliers are relatively inexpensive, compact, light-weight and reliable compared to vacuum tube technology, which makes them suitable for space applications.

Frequency multiplication or harmonic generation in devices occur due to their non-linearity. Depending on if the multiplication is due to a non-linear resistance or a non-linear reactance, one differ between the varistor or varactor type of multiplier. Varactor type multipliers have high potential conversion efficiency, but exhibit a narrow bandwidth and a high sensitivity to operating conditions. According to the Page-Pantell inequality, multipliers that depend upon a non-linear resistance have at most an efficiency of $1/n^2$, where n is the order of multiplication [Page 1958; Pantell 1958]. Absence of reactive energy storage in varistor frequency multipliers ensures large bandwidth. For the ideal varactor multiplier, i.e. a lossless non-linear reactance, the theoretical limit is a conversion efficiency of 100 %. However, in reality properties and parameters are a mixture of the ideal varistor and the ideal varactor multiplier. Basic varactor frequency multiplier theory is described in the books by Penfield and Rafuse [1962], Faber *et al.* [1995] and the paper by Burckhardt [1965]. The following set of parameters are used to describe and compare properties of frequency multipliers:

Idler circuit

The term idler circuit is used to describe circuits at frequencies (except input/output frequencies) that are essential for multiplier performance.

Conversion loss

Conversion loss, L_n, is defined as the ratio of the available source power, P_{AVS}, to the output harmonic power, P_n, delivered to the load resistance. It is usually expressed in decibels. The inverted value of, L_n, i.e. the conversion efficiency, η_n, is often expressed in percent.

Source and load impedance

In order to minimise the conversion loss, optimum source, Z_S, and load, Z_L, embedding impedances should be provided to the diode. Optimum source and load impedances are found from maximising, e.g. the conversion efficiency, and they depend on each other and on the input signal level. In a non-linear circuit, such as a multiplier, it is not possible to define a true impedance. However, a "quasi-impedance", Z_n, can be defined for periodic signals as

$$Z_n = \frac{V_n}{I_n} \tag{13}$$

where V_n and I_n are the voltage and the current, respectively, at the n^{th} harmonic.

3.1 Basic principles of single diode frequency multipliers

Single diode frequency multipliers can either be shunt or series mounted. In both cases the input and the output filter should provide optimum embedding impedances at the input and output frequencies, respectively. The output filter should also provide an open circuit for the shunt mounted diode and a short circuit for the series mounted varactor at the pump frequency. The same arguments are true for the input filter at the output frequency.

Besides the above conditions, the correct impedances must be provided at the idler frequencies for a high order multiplier (e.g. a quintupler). In general, it is hard to achieve optimum impedances at the different harmonics simultaneously. Therefore, a compromise has to be found.

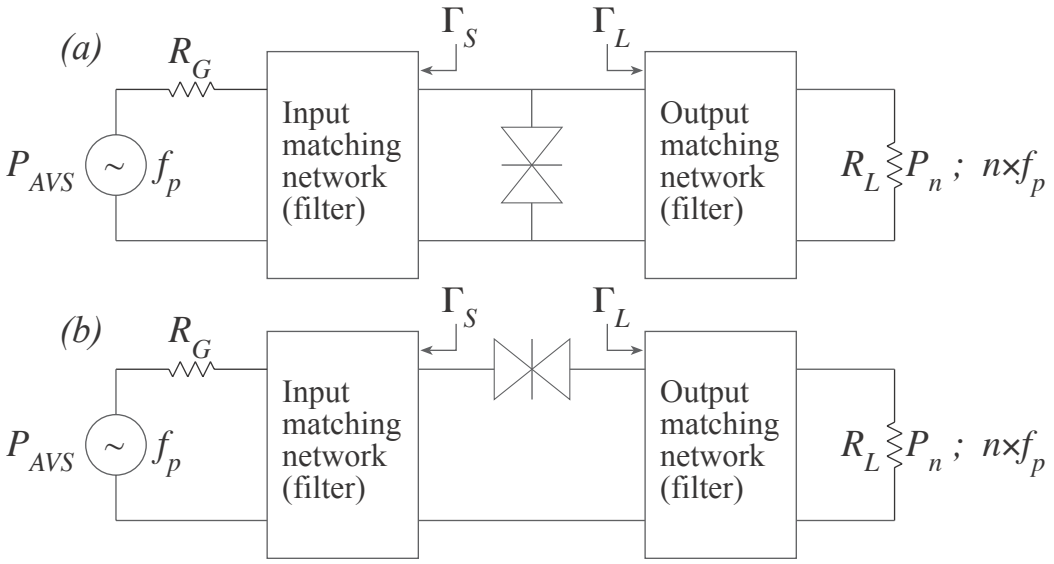

Figure 13: Block scheme of n^{th}-order frequency multiplier circuit with (a) shunt mounted and (b) series mounted diodes.

3.2 Analysis of symmetric varactor frequency multipliers

Single tone excitation of strongly non-linear circuits, such as frequency multipliers, is normally analysed by means of the harmonic balance technique [e.g. Maas 1988]. A convenient approach, originally introduced by Tang [1966], is to describe the non-linear S-V characteristic with a polynomial V-Q model and using Uhlir's varactor model (Figure 4). Tang's approach was first applied to symmetric varactors by Krishnamurthi *et al.* [1993] with a cubic polynomial V-Q model. For the tripler, Krishnamurthi *et al.* present analytical expressions for the optimal embedding impedances and the maximum conversion efficiency. A simple set of accurate design equations that can be used to calculate impedances, input power and RF efficiency for HBV triplers are presented in reference [Stake 1999a].

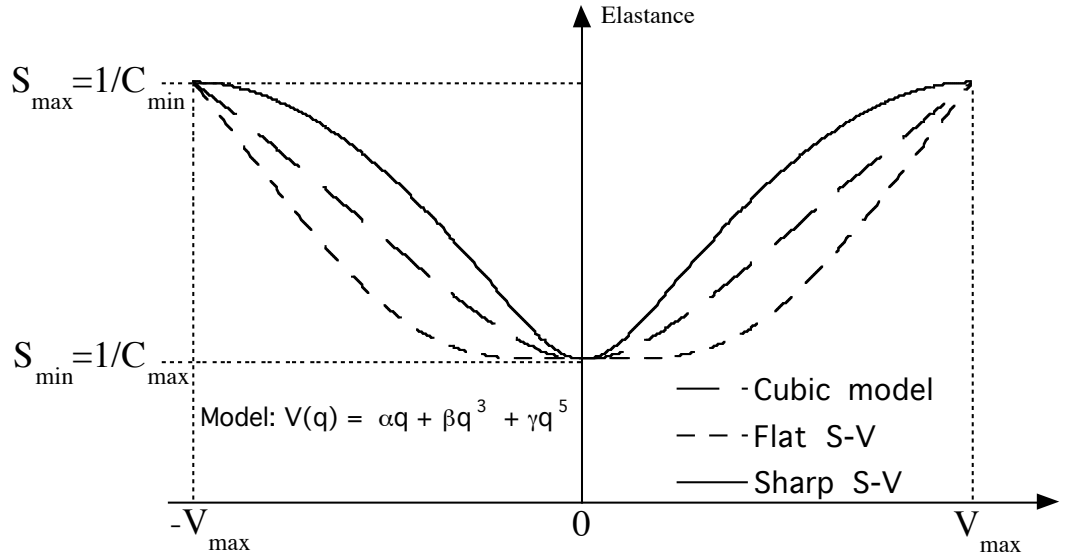

Figure 14: Different S-V characteristics generated from a fifth degree polynomial model.

To systematically investigate how the tripler and quintupler performance depends on the shape of the S-V characteristic, a fifth degree polynomial model can be employed (Figure 14) [Kollberg 1996; Dillner 1997a]. In Figure 15 a calculation of the minimum conversion loss for a tripler and a quintupler is shown. The best efficiency is obtained for a S-V characteristic with large non-linearity at zero volt. The optimum idler circuit for the quintupler is an inductance in resonance with the diode capacitance (i.e. maximised third harmonic current).

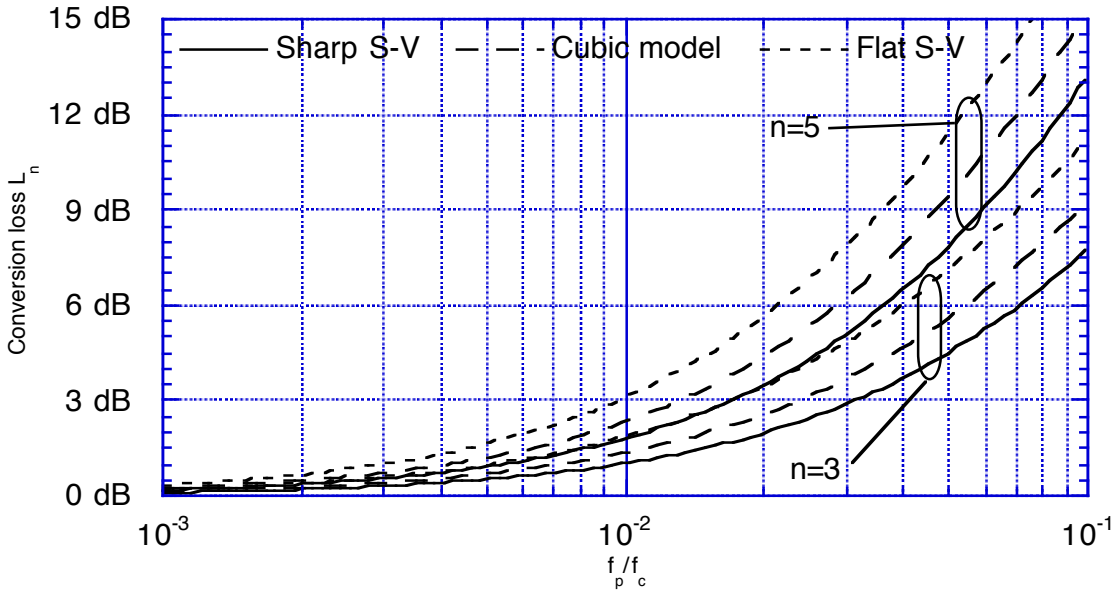

Figure 15: The minimum conversion loss for a tripler and a quintupler for the different S-V characteristics shown in Figure 14. The pump frequency is normalised with the dynamic cut-off frequency (1). For the quintupler case, the idler circuit is an inductance in resonance with the diode capacitance.

3.3 Carrier transport during RF-operation

A time-dependent numerical Drift/Diffusion device model integrated with a large signal Harmonic Balance circuit simulator (DDHB) has been developed by Jones *et al.* [Jones 1995a; Jones 1995b]. Carrier transport is modeled by solving the electron continuity equation (14), the drift/diffusion equation (15), and the Poisson equation (16) self-consistently. The resulting equations describing DC and time dependent transport are formulated as

$$\frac{\partial n(x,t)}{\partial t} = \frac{1}{q}\frac{\partial J_n(x,t)}{\partial x}, \tag{14}$$

$$J_n(x,t) = -q\mu_n(x,t)\,n(x,t)\frac{\partial \phi_n(x,t)}{\partial x}, \tag{15}$$

and

$$\frac{\partial}{\partial x}\left[\varepsilon(x)\frac{\partial \psi(x,t)}{\partial x}\right] = q\left[n(x,t) - N_D(x)\right], \tag{16}$$

where

$$n(x,t) = n_{i,ref}\, e^{\frac{q}{kT}\left(\psi(x,t)+V_n(x)-\phi_n(x,t)\right)}, \tag{17}$$

and where J_n is the electron current density, n is the electron density, ϕ_n is the electron quasi-Fermi potential, ψ is the electrostatic potential, k is Boltzmann's constant, q is the electron charge, T is the absolute temperature, $n_{i,ref}$ is the intrinsic electron density in the reference material (GaAs), and V_n, μ_n, N_D, and ε are the spatially-dependent alloy potential, electron mobility, donor impurity concentration, and dielectric permittivity, respectively. The conduction band, the eletcric field and the carrier concentration for the HBV in Table III are shown in Figure 17 and Figure 18. The embedding impedances were optimised for maximum efficiency [see Stake 1997]. Calculations were performed for a four-barrier structure, device area of 66 μm^2, and an extrinsic parasitic series resistance of 5 ohm. The current versus voltage during one pump cycle for two different drive levels are shown in Figure 16. An increased carrier concentration can be observed in the depleted region due to the onset of large conduction current through the barrier for high voltages, see Figure 18.

To observe the effect of current saturation, a field-dependent model should be added. However, an accurate model for carrier transport at high frequencies should include the effect of hot electron transport. In this case, a Monte-Carlo description of carriers is needed [Lipsey 1997] or energy balance equations should be included in the above model [Hjelmgren 1991].

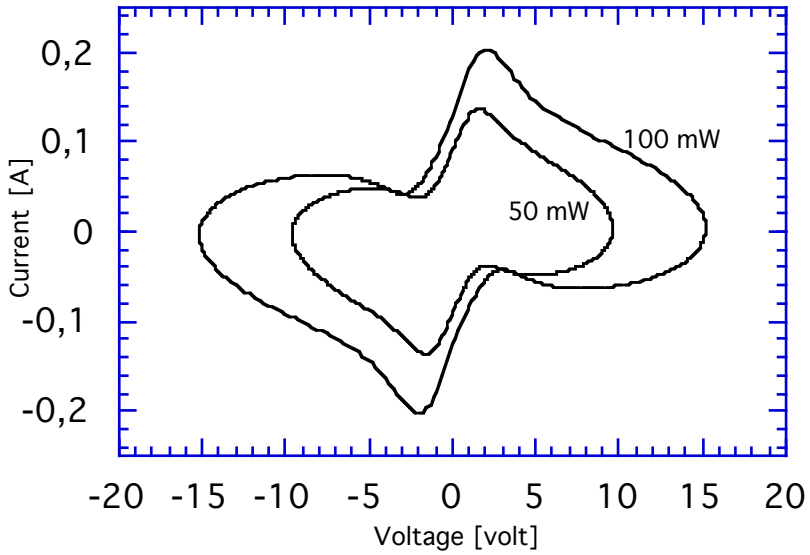

Figure 16: *Current versus voltage during one pump-cycle for an input power of 50 mW and 100 mW at 90 GHz.*

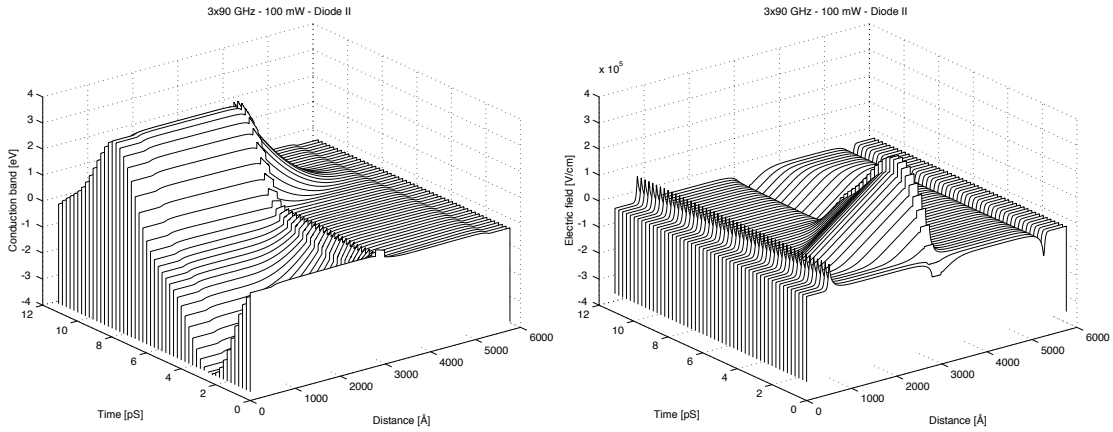

Figure 17: *The conduction band (left) and the electric field (right) versus time and distance for an incident pump power of 100 mW @ 90 GHz.*

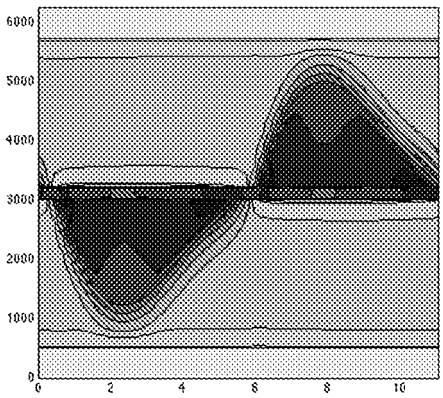

Figure 18: *Contour plot (log scale) of carrier concentration versus time and distance for an incident pump power of 100 mW @ 90 GHz. Contour lines are at a carrier density of 10^{11}, 10^{12}, 10^{13}, 10^{14}, 10^{15}, 10^{16}, 5×10^{16}, 10^{17}, 5×10^{17} and 10^{18} cm^{-3}, respectively.*

3.4 Practical HBV multipliers

Since frequency multipliers find applications mostly as sources at higher millimetre and submillimetre wave frequencies, they are often realised in waveguide mounts. A classic design is the arrangement of crossed rectangular waveguides of widths specific for the input and output frequency bands (Figure 19). The advantages are:

- The input signal does not excite the output waveguide, which is cut-off at the input frequency.
- Low losses.
- The height of the waveguide in the diode mounting plane may be chosen to provide the electrical matching conditions. Assuming a thin planar probe, the output embedding impedance is given by analytical expressions [Eisenhart 1971].
- Movable short circuits provide input/output tunability.

Today, whole waveguide mounts can be analysed and designed using commercial available high frequency electromagnetic CAD tools. They either solve Maxwell's equations in the frequency domain (HP-HFSS) or in the time-domain using the FDTD method.

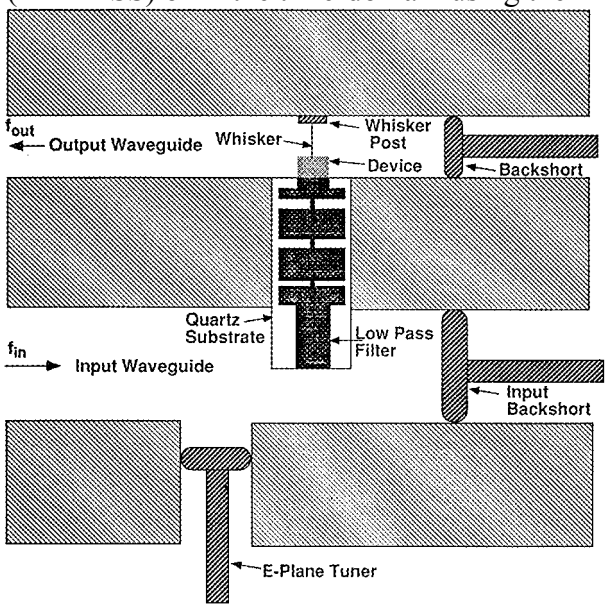

Figure 19: Schematic diagram of a crossed waveguide mount [from Choudhury 1993]. The output signal is isolated from the input waveguide with a low pass filter.

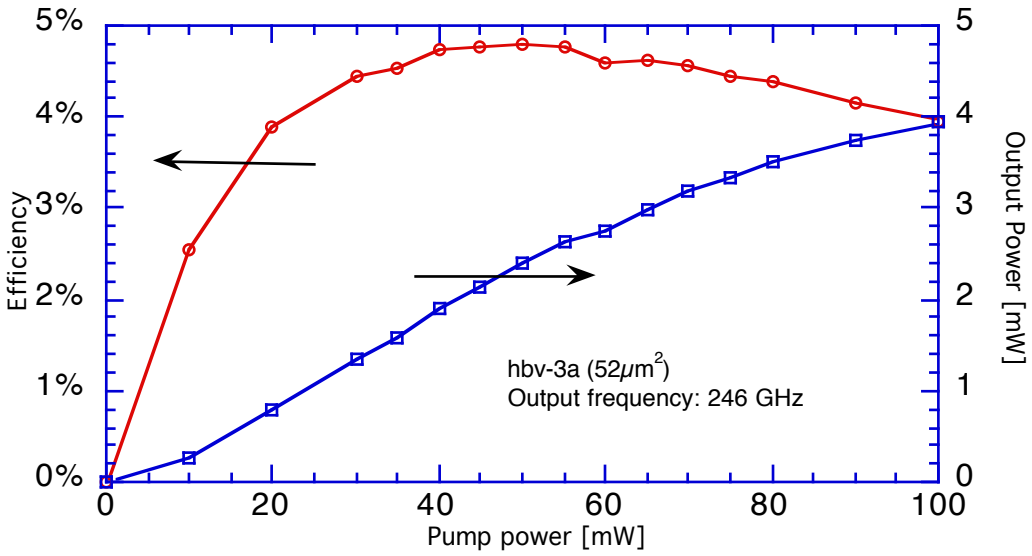

Figure 20: *Measured output power and conversion efficiency for a four barrier AlGaAs HBV (CTH-NU2003J).*

The performance of a four-barrier AlGaAs HBV tripler at 246 GHz is shown in Figure 20. The planar diode was mounted across the output waveguide in a crossed waveguide type of multiplier block (RAL-HBVII). The waveguide is equipped with two input tuners and two output tuners. Input power was provided by a J.E. Carlstrom (H270) GUNN oscillator. The efficiency saturates for an input power of 50 mW due to the effect of self-heating. As thermionic emission dominates the electron transport across the barrier of standard AlGaAs HBVs, the conduction current increases drastically with temperature and hence a reduced conversion efficiency.

Table IV briefly reviews the status of HBV multipliers and how they compare with some representative Schottky multipliers.

The machining and assembly problems increase rapidly above ~300 GHz for waveguide mounts. Single mode operation becomes a problem at these frequencies and at very high frequencies (1 THz) the cost of waveguide components will be too high for use in most systems. Therefore, the quasi-optical approach [Goldsmith 1998] is very useful for single diode submillimetre wave multipliers. Low loss free space power propagation is coupled to the diode through an integrated antenna.

Table IV: Performance of some representative HBV and Schottky multipliers

Varactor Frequency Multipliers				
$n \times f_p$ [GHz]	Efficiency [%]	Output power [mW]	Reference	Comments
92	10	91	Rahal [1995]	InP, 10 barrier HBV
141	8,1	11,5	Hollung [1999b]	GaAs, 2x2 barrier HBV, Quasi-optical
171	0,78	0,02	Räisänen, [1995]	InP, 1 barrier HBV Quin-tupler
174	22	55	Rizzi [1993]	Schottky balanced doubler
216	5.4	5	Mélique [1998b]	InP, 2x2 barrier HBV, 48 μm^2
222	5	1	Rydberg, [1990]	GaAs, 1 barrier HBV, 7μm^2
246	4,8	4	Stake [1999b]	GaAs, 2x2 barrier HBV, 52μm^2
247,5	12	8,9	Mélique [1999]	InP, 2x2 barrier HBV, 28 μm^2
271	9	15	Thornton [1998]	Schottky tripler
332	20	4	Erickson [1990]	Schottky balanced doubler
498	3	0,7	Erickson [1990]	Schottky tripler
800	3	0,25	Crowe [1996]	Schottky tripler

The quasi-optical approach, i.e. when geometrical (ray) optics approximation is invalid, becomes important when the beam diameter becomes smaller than 100 wavelengths. A Gaussian beam is normally launched through a corrugated horn and further processed by means of beam splitters, lenses, diplexers and interferometers.

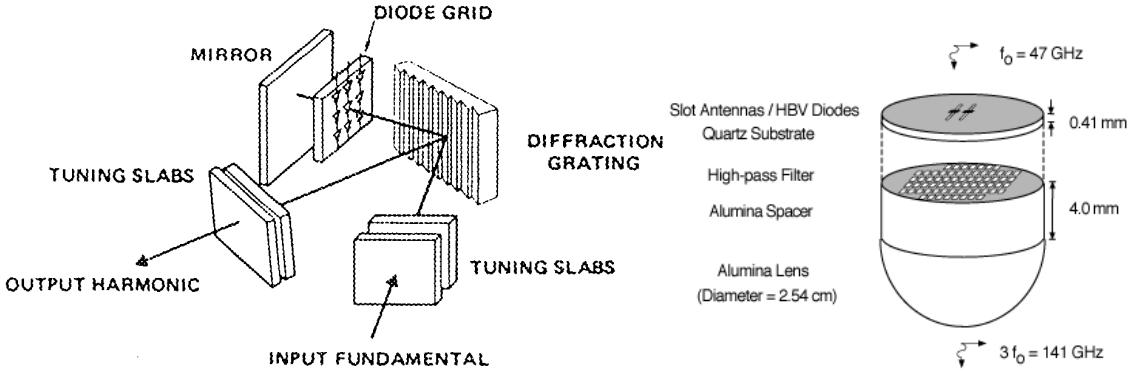

Figure 21: Two different quasi-optical millimetre wave diode frequency multipliers. A diode grid (Left) [from Hwu 1989] and a HBV tripler (right) [Hollung 1999a]

In the millimetre wave region, power combining through a grid of varactor diodes can provide several watts of output power. The power illuminating the grid is distributed among the diodes, and power generated at a desired harmonic is then recombined in a quasi-optical structure (Figure 21).

4. Summary of appended papers

Nine papers (A-I) are appended in this thesis. They are grouped according to their content: multiplier testing and the effect of heating (A-C), modelling and analysis (D-F), and HBV fabrication and diode characterisation (H, I).

Paper A reports work on the effect of self-heating in planar HBVs.

Paper B reports new tripler results with GaAs/AlGaAs based HBVs.

Paper C proposes a novel fabrication process for HBVs on copper substrate.

Paper D proposes a simple set of HBV tripler design equations.

Paper E reports analysis of symmetric varactor multipliers.

Paper F reports work on optimisation of the HBV barrier structure.

Paper G reports a 141 GHz quasi-optical HBV tripler circuit.

Paper H reports an on-wafer high frequency C-V characterisation method.

Paper I describes the technology used for fabrication and characterisation of HBVs at Chalmers.

5. Concluding remarks

Several projects are in progress with the intention of implementing short millimetre waves for short distance communication. Furthermore, a Swedish satellite (ODIN) for studying global ozone depletion will carry three submillimetre wave radiometers (120, 480 and 550 GHz). These systems demand efficient, pure and high power sources. The lack of good solid state sources in the submillimetre wavelength range motivates research on high efficiency varactor multipliers and novel fundamental oscillators (e.g. Bloch oscillators, p-Ge lasers etc.).

III-V compounds (e.g. InGaAs) are promising materials for submillimetre wave applications. However, development of new materials such as wide band gap materials (e.g. nitrides, carbides) can also provide solutions for high power sources in the millimetre wave region.

Novel multiplier topologies, which take advantage of the symmetry of the HBV, will be developed. A compact circuit realisation is necessary for monolithical technology. High conversion efficiency and high output power by means of epitaxially stacked barriers is no longer a utopia and the performance is comparable to the Schottky diode. Furthermore, the grids and quasi-optical systems can provide several watts of output power. A transmission line periodically loaded with HBVs (NLTL), where a soliton can propagate, could provide a trade-off between multiplier-efficiency and bandwidth [e.g. Li 1998].

To make terahertz applications more cost effective, material techniques and processing techniques must be further developed. A development towards a monolithic approach, i.e., low loss transmission media, airbridges, antennas etc. on the chip, is therefore necessary. Moreover, simulation and synthesis tools must be improved at these frequencies.

The demand of sensitive heterodyne receivers and broadband communication systems will push the material and fabrication technology forward in the years to come. The HBV diode will play an important role in this development.

6. Acknowledgements

First I would like to thank my supervisor, Professor Erik Kollberg, for his encouragement, support and for giving me the opportunity to perform this work. I really appreciate the fruitful discussions we have had about new ideas and problems. Many thanks to Professor Lennart Lundgren, who was my first contact with the millimetre wave group at Chalmers, for his support, encouragement, and careful reading of numerous manuscripts, and especially for giving me the great opportunity and responsibility to teach the course "Active Microwave Circuits".

Professor Stephen Jones, who made my five months at the University of Virginia unforgettable. His enthusiasm and scientific skills have really inspired me.

Dr. Chris Mann at the Rutherford Appleton Laboratory for his support and encouragement, and for all hard work he has done on multiplier assembling and testing. I would also like to acknowledge the rest of the staff at the Millimetre Wave Technology group.

My HBV colleagues: Tekn. Lic. Lars Dillner, Dr. Stein Hollung, and Mattias Ingvarson for their support and the enjoyable time we have had together. Without them, this work would be nothing.

I would like to thank the staff at the millimetre wave group at Chalmers: Tekn. Lic. Klas Yhland, Dr. Niklas Rorsman, Dr. Erik Carlsson, Dr. Christer Karlsson, Dr. Peter Petrov, Dr. Shumin Wang, Dr. Hans Grönqvist, Fariba Ferdos, Joakim Eriksson, Dr. Ilcho Angelov and Dr. Piotr Starski whom I have had the benefit of working together with during my time as a PhD student. The work would have been naught without the administrative and technical personnel: Bente Larsson, Lillemor Bergström, Salah Kesraoui, Jan Andersson, Anders Olausson and Emmanuil Choumas. Many thanks to Göran Reivall for his support and his skills that keeps the III-V lab running.

The co-operation with Prof. Magnus Willander and Dr. Ying Fu at the department of Physical Electronics and Photonics at Chalmers.

All participants in the ESPRIT basic research project "PARTNERS". Especially, Dr. Kristel Fobelets, Dr. Chris Van Hoof, Prof. Gustaaf Borghs and Prof. Koung-An Chao for good co-operation. All participants within the ESA project Millimetre Wave Sounders Critical Technology: Prof. Didier Lippens, Reynald Havart, Jorge Carbonell, Prof. Gérard Beaudin, Fernando Gomez and Prof. Jean-Marc Goutoule for good co-operation.

This work has been supported by the SSF High Speed Electronics program and the ESPRIT basic research project "PARTNERS". My research visit to University of Virginia was partly supported by grants from LM Ericsson and the Royal Swedish Academy of Sciences.

Finally, I would like to thank my friends and relatives for their patience and support during this work, and for giving me a life beyond Chalmers.

7. References

[Adamski 1998] M.E. Adamski, M.T. Faber and J.A. Dobrowolski, "Heterostructure Barrier Varactor Multiplier Simulation Using Physics Based Quasi-Static Charge Model," 28th European Microwave Conference, Amsterdam, pp. 146-151, 1998.

[Batey 1986] J. Batey and S.L. Wright, "Energy band alignment in GaAs: (Al, Ga)As heterojunctions: The dependence on alloy composition," *J. Appl. Phys.*, vol. 59, pp. 200-209, 1986.

[Bishop 1987] W.L. Bishop, K. McKiney, R.J. Mattauch, T.W. Crowe and G. Green, "A Novel Whiskerless Schottky Diode for Millimeter and Submillimeter Wave Applications," 1987 IEEE MTT-S International Microwave Symposium Digest, Las Vegas, pp. 607-610, 1987.

[Burckhardt 1965] C.B. Burckhardt, "Analysis of Varactor Frequency Multipliers for Arbitrary Capacitance Variation and Drive Level," *The Bell System Technical Journal*, pp. 675-692, 1965.

[Cho 1983] A.Y. Cho, "Molecular Beam Epitaxy Growth of III-V semiconductor and their properties," *Thin Solid Films*, vol. 100, pp. 291-, 1983.

[Choudhury 1993] D. Choudhury, M.A. Frerking and P.D. Batelaan, "A 200-GHz tripler using a single barrier varactor," *IEEE Trans. Microwave Theory Tech.*, vol. 41, pp. 595-599, 1993.

[Crowe 1996] T.W. Crowe, T.C. Grein, R. Zimmermann and P. Zimmermann, "Progress Toward Solid-State Local Oscillators at 1 THz," *IEEE Microwave Guided Wave Lett.*, vol. 6, pp. 207-208, 1996.

[Crowe 1997] T.W. Crowe, P.J. Koh, W.L. Bishop and C.M. Mann, "Inexpensive Receiver Components for Millimeter Wavelengths," Eighth International Symposium on Space Terahertz Technology, Boston, pp. 377-384, 1997.

[Crowe 1995] T.W. Crowe, R.J. Mattauch, R.M. Weikle and U.V. Bhapkar, "Terahertz GaAs Devices and Cirquits for Heterodyne Receiver applications," *International Journal of High Speed Electronics and Systems*, vol. 6, pp. 125-161, 1995.

[Dickens 1967] L.E. Dickens, "Spreading Resistance as a Function of Frequency," *IEEE Trans. on Microwave Theory and Techniques*, vol. 15, pp. 101-109, 1967.

[Dillner 1997a] L. Dillner, J. Stake and E.L. Kollberg, "Analysis of Symmetric Varactor Frequency Multipliers," *Microwave Opt. Technol. Lett.*, vol. 15, pp. 26-29, 1997a.

[Dillner 1997b] L. Dillner, J. Stake and E.L. Kollberg, "Modeling of the Heterostructure Barrier Varactor Diode," 1997 International Semiconductor Device Research Symposium, Charlottesville, pp. 179-182, 1997b.

[Dillner 1999] L. Dillner, J. Stake and E.L. Kollberg, "Heterostructure Barrier Varactors on Copper Substrate," *Electronics Letters*, vol. 35, 1999.

[Duez 1998] V. Duez, X. Mélique, O. Vanbésien, P. Mounaix, F. Mollot and D. Lippens, “High capacitance ratio with GaAs/InGaAs/AlAs heterostucture quantum well-barrier varactors,” *Electronic Letters*, vol. 34, pp. 1860-1861, 1998.

[Dupuis 1984] D. Dupuis, “Chemical Vapor Deposition for III-V Compound Semiconductor Devices,” Int. Conf. on Chemical Vapor Deposition, Cincinnati, pp. 503-516, 1984.

[Eisenhart 1971] E.L. Eisenhart and P.J. Khan, “Theoretical and Experimental Analysis fo a Waveguide Mounting Structure,” *IEEE Transaction on Microwave Theory and Techniques*, vol. 19, 1971.

[Erickson 1990] N.R. Erickson, “High Efficiency Submillimeter Frequency Multipliers,” IEEE MTT-S, Dallas, pp. 1301-1304, 1990.

[Faber 1995] M.T. Faber, J. Chramiec and M.E. Adamski, *Microwave and Millimeter-Wave Diode Frequency Multipliers*. Boston: Artech House Publishers, 1995.

[Fu 1998] Y. Fu, L. Dillner, J. Stake, M. Willander and E.L. Kollberg, “Capacitance Analysis for AlGaAs/GaAs and InAlAs/InGaAs Heterostructure Barrier Varactor Diodes,” *J. Appl. Phys.*, vol. 83, pp. 1457-1462, 1998.

[Fu 1997] Y. Fu, J. Stake, L. Dillner, M. Willander and E.L. Kollberg, “AlGaAs/GaAs and InAlAs/InGaAs Heterostructure Barrier Varactors,” *J. Appl. Phys.*, vol. 82, pp. 5568-5572, 1997.

[Fu 1999] Y. Fu, J. Stake, L. Dillner, M. Willander and E.L. Kollberg, “Carrier Conduction in a Heterostructure Barrier varactor Induced by an AC-Bias,” *submitted to the J. Appl. Phys.*, 1999.

[Goldsmith 1998] P.F. Goldsmith, *Quasioptical Systems*. Piscataway, NJ: IEEE Press, 1998.

[Hjelmgren 1991] H. Hjelmgren, “Numerical Modelling of Hot Electron Transport in Schottky-diodes and Heterojunction Structures,” *Ph.D. Thesis, Department of Radio and Space Science*, Chalmers University of Technology, Göteborg, 1991.

[Hollung 1999a] S. Hollung, J. Stake, L. Dillner and E.L. Kollberg, “A 141-GHz Integrated Quasi-Optical Slot Antenna Tripler,” submitted to the IEEE AP-S International Symposium and USNC/URSI National Radio Science Meeting, Orlando, 1999a.

[Hollung 1999b] S. Hollung, J. Stake, L. Dillner and E.L. Kollberg, “A 141-GHz Quasi-Optical HBV Diode Frequency Tripler,” Tenth International Symposium on Space Terahertz Technology, Charlottesville, 1999b.

[Hwu 1989] R.J. Hwu, “Quasi-Optical Watt-Level Millimeter-Wave Monolithic Solid-State Diode-Grid Frequency Multipliers,” IEEE MTT-S Int. Microwave Symp. Digest, Long Beach, pp. 1069-1072, 1989.

[Inoue 1991] K. Inoue, J.C. Harmand and T. Matsuno, “High-quality $In_xGa_{1-x}As$/InAlAs modulation doped heterostructures grown lattice-mismatched on GaAs substrates,” *Journal of Crystal Growth*, pp. 313-317, 1991.

[Jones 1997] J.R. Jones, W.L. Bishop, S.H. Jones and G.B. Tait, "Planar Multi-Barrier 80/240 GHz Heterostructure Barrier Varactor Triplers," *IEEE Trans. Microwave Theory Tech.*, vol. 45, pp. 512-518, 1997.

[Jones 1994a] J.R. Jones, S.H. Jones and G.B. Tait, "GaAs/InGaAs/AlGaAs Heterostructure Barrier Varactors for Frequency Tripling," Fifth International Symposium on Space Terahertz Technology, Ann Arbor, Michigan, pp. 497-513, 1994a.

[Jones 1995a] J.R. Jones, S.H. Jones and G.B. Tait, "Self-Consistent Physics-Based Numerical Device/Harmonic-Balance Circuit Analysis of Heterostructure Barrier Varactors Including Thermal Effects," Sixth International Symposium on Space Terahertz Technology, Pasadena, California, pp. 423-441, 1995a.

[Jones 1994b] J.R. Jones, S.H. Jones, G.B. Tait and M.F. Zybura, "Heterostructure Barrier Varactor Simulation Using an Integrated Hydrodynamic Device/Harmonic-Balance Circuit Analysis Technique," *IEEE Microwave Guided Wave Lett.*, vol. 4, pp. 411-413, 1994b.

[Jones 1995b] J.R. Jones, G.B. Tait, S.H. Jones and S.D. Katzer, "DC and Large-Signal Time-Dependent Electron Transport in Heterostructure Devices: An Investigation of the Heterostructure Barrier Varactor," *IEEE Trans. Electron Devices*, vol. 42, pp. 1393-1403, 1995b.

[Katz 1992] A. Katz, Ed. Indium Phosphide and Related Materials: Processing, Technology, and Devices. Boston, Artech House. 1992.

[Kollberg 1989] E.L. Kollberg and A. Rydberg, "Quantum-barrier-varactor diode for high efficiency millimeter-wave multipliers," *Electron. Lett.*, vol. 25, pp. 1696-1697, 1989.

[Kollberg 1996] E.L. Kollberg, J. Stake and L. Dillner, "Heterostructure barrier varactors at submillimetre waves," *Phil. Trans. R. Soc. Lond. A*, vol. 354, pp. 2383-2398, 1996.

[Kollberg 1992] E.L. Kollberg, T.J. Tolmunen, M.A. Frerking and J.R. East, "Current Saturation in Submillimeter Wave Varactors," *IEEE Trans. Microwave Theory Tech.*, vol. 40, pp. 831-838, 1992.

[Krishnamurthi 1993] K. Krishnamurthi and R.G. Harrison, "Analysis of Symmetric-Varactor Frequency Triplers," IEEE-MTT Int. Microwave Symp. Digest, pp. 649-652, 1993.

[Krishnamurthi 1994] K. Krishnamurthi, S.M. Nilsen and R.G. Harrison, "GaAs Single-Barrier Varactors for Millimeter-Wave Triplers: Guidelines for Enhanced Performance," *IEEE Trans. Microwave Theory Tech.*, vol. 42, pp. 2512-2516, 1994.

[Kroemer 1992] H. Kroemer, C. Nguyen and B. Brar, "Are there Tamm-state donors at the InAs-AlSb quantum well interface," *Journal of Vacuum Science and Technology B*, vol. 10, pp. 1769-1772, 1992.

[Landheer 1989] D. Landheer, H.C. Liu, M. Buchanan and R. Stoner, "Tunneling through AlAs barriers: Γ–X transfer current," *Appl. Phys. Lett.*, vol. 54, pp. 1784-1786, 1989.

[Lheurette 1998] E. Lheurette, X. Mélique, P. Mounaix, F. Mollot, O. Vanbésien and D. Lippens, "Capacitance Engineering for InP-Based Heterostructure Barrier Varactor," *IEEE Electron Dev. Lett.*, vol. 19, pp. 338-340, 1998.

[Lheurette 1996] E. Lheurette, P. Mounaix, P. Salzenstein, F. Mollot and D. Lippens, "High Performance InP-based Heterostructure Barrier Varactors in Single and Stack Configuration," *Electronics Letters*, vol. 32, pp. 1417-1418, 1996.

[Li 1998] M. Li and R.G. Harrison, "A Fully-Distributed Heterostructure-Barrier-Varactor Nonlinear-Transmission-Line Frequency Tripler," IEEE-MTT Int. Microwave Symp. Digest, Baltimore, pp. 1639-1642, 1998.

[Lieneweg 1992] U. Lieneweg, T.J. Tolmunen, M.A. Frerking and J. Maserjian, "Modeling of Planar Varactor Frequency Multiplier Devices with Blocking Barriers," *IEEE Trans. Microwave Theory Tech.*, vol. 40, pp. 839-845, 1992.

[Lipsey 1997] R.E. Lipsey, S.H. Jones, J.R. Jones, L.F. Horvath, U.V. Bhapkar, T.W. Crowe and R.J. Mattauch, "Monte Carlo Harmonic-Balance and Drift-Diffusion Harmonic-Balance Analyzes of 100-600 GHz Schottky Barrier Varactor Frequency Multipliers," *IEEE Trans. on Electron Devices*, vol. 44, pp. 1843-1849, 1997.

[Louhi 1995] J.T. Louhi and A.V. Räisänen, "On the Modeling and Optimisation of Schottky Varactor Frequency Multipliers at Submillimeter Wavelengths," *IEEE Trans. Microwave Theory Tech.*, vol. 43, pp. 922-926, 1995.

[Lubecke 1998] V.M. Lubecke, C.M. Mann and K. Mizuno, "Practical Micromachining Techniques for High Aspect Ratio Submillimeter Wave Components," Ninth International Symposium on Space Terahertz Technology, Pasadena, CA, pp. 425-429, 1998.

[Maas 1988] S.A. Maas, *Nonlinear Microwave Circuits*: Artech House, 1988.

[Madelung 1991] O. Madelung, Ed. Semiconductors: Group IV Elements and III-V Compounds. Berlin, Springer-Verlag. 1991.

[Mahiey 1998] S. Mahiey, C.M. Mann, J. Stake, L. Dillner, S.H. Jones and J. Thornton, "A Broadband Frequency Tripler for SIS Receivers," Ninth International Symposium on Space Terahertz Technology, Pasadena, 1998.

[Mann 1997] C.M. Mann, "Integrated Waveguides and Mixers," in *New Directions in Terahertz Technology*, *Applied Sciences-Vol. 334*, J. M. Chamberlain and R. E. Miles, Eds. London: Kluver Academic Publishers, pp. 175-191, 1997.

[Mélique 1998a] X. Mélique, J. Carbonell, R. Havart, P. Mounaix, O. Vanbésien and D. Lippens, "InGaAs/InAlAs/AlAs Heterostructure Barrier Varactors for Harmonic Multiplication," *IEEE Microwave and Guided Wave Letters*, vol. 8, pp. 254-256, 1998a.

[Mélique 1999] X. Mélique, A. Maestrini, E. Lheurette, P. Mounaix, M. Favreau, O. Vanbésien, J.M. Goutoule, G. Beaudin, T. Nähri and D. Lippens, "12% Efficiency and 9.5 dBm Output Power from InP-based Heterostructure Barrier varactor Triplers at 250 GHz," IEEE-MTT Int. Microwave Symposium, Anaheim, 1999.

[Mélique 1998b] X. Mélique, C.M. Mann, P. Mounaix, J. Thornton, O. Vanbésien, F. Mollot and D. Lippens, "5 mW and 5 % Efficiency 216 GHz InP-based Heterostructure Barrier Varactor Tripler," *IEEE Microwave and Guided Wave Letters*, vol. 8, pp. 384-386, 1998b.

[Mishima 1995] T. Mishima, K. Higuchi, M. Mori and M. Kudo, "High G_m $In_{0.5}Al_{0.5}As/In_{0.5}Ga_{0.5}As$ high electron mobility transistors grown lattice-mismatched on GaAs substrates," *Journal of Crystal Growth*, pp. 1230-1235, 1995.

[Mönch 1993] W. Mönch, *Semiconductor Surfaces and Interfaces*: Springer-Verlag, 1993.

[Nilsen 1994] S.M. Nilsen, "III-V Semiconductor device fabrication procedures and process simulations," Chalmers University of Technology, Department of Microwave Technology, Göteborg, Technical Report No. 7, January 1994.

[Nilsen 1992] S.M. Nilsen, H. Grönqvist, H. Hjelmgren, A. Rydberg and E.L. Kollberg, "Progress on Single Barrier Varactors for Submillimeter Wave Power Generation," Third International Symposium on Space Terahertz Technology, Michigan, 1992.

[Oswald 1998] J.E. Oswald, T. Koch, I. Mehdi, A. Pease, R.J. Dengler, T.H. Lee, D.A. Humphrey, M. Kim, P.H. Siegel, M.A. Frerking and N.R. Erickson, "Planar Diode Solid-State Receiver for 557 GHz with State-of-the-Art Performance," *IEEE Microwave and Guided Wave Letters*, vol. 8, pp. 232-234, 1998.

[Page 1958] C.H. Page, "Harmonic generation with ideal rectifiers," *Proceedings IRE*, vol. 46, pp. 1738-1740, 1958.

[Pantell 1958] R.H. Pantell, "General power relationship for positive and negative nonlinear resistive elements," *Proceedings IRE*, vol. 46, pp. 1910-1913, 1958.

[Peatman 1992] W.C.B. Peatman, T.W. Crowe and M. Shur, "A Novel Schottky/2-DEG Diode for Millimeter- and Submillimeter-Wave Multiplier Applications," *IEEE Electron Device Lett.*, vol. 13, pp. 11-13, 1992.

[Penfield 1962] P. Penfield and R.P. Rafuse, *Varactor Applications*. Cambridge: M.I.T. Press, 1962.

[Rahal 1995] A. Rahal, E. Boch, C. Rogers, J. Ovey and R.G. Bosisio, "Planar multi-stack quantum barrier varactor tripler evaluation at W-band," *Electronics Letters*, vol. 31, pp. 2022-2023, 1995.

[Rizzi 1993] B.J. Rizzi, T.W. Crowe and N.R. Erickson, "A High-Power Millimeter-Wave Frequency Doubler Using a Planar Diode Array," *IEEE Microwave and Guided Wave Letters*, vol. 3, pp. 188-190, 1993.

[Rohdin 1995] H. Rohdin, A. Nagy, V. Robbins, C. Su, C. Madden, A. Wakita, J. Raggio and J. Seeger, "Low-Noise, High Speed GaInAs/AlInAs 0.1 μm MODFETs and High-Gain/Bandwidth Three-Stage Amplifier Fabricated on GaAs Substrate," IEEE 7th International Conference on Indium Phosphide and Related Materials, Sapporo, Japan, pp. 73-76, 1995.

[Rorsman 1992] N. Rorsman, C. Karlsson and H. Zirath, "Fabrication and Characterisation of Heterostructure Field Effect Transistors," Chalmers University of Technology, Department of Applied Electron Physics, Göteborg, Technical Report No. 61 (Revised), May 1992.

[Ruch 1970] J.G. Ruch and W. Fawcett, "Temperature Dependence of the Transport Properties of Gallium Arsenide Determined by a Monte Carlo Method," *J. Appl. Phys.*, vol. 41, pp. 3843-3849, 1970.

[Rydberg 1990] A. Rydberg, H. Grönqvist and E.L. Kollberg, "Millimeter- and Submillimeter-Wave Multipliers Using Quantum-Barrier-Varactor (QBV) Diodes," *IEEE Trans. Electron Devices*, vol. 11, pp. 373-375, 1990.

[Räisänen 1995] A.V. Räisänen, T.J. Tolmunen, M. Natzic, M.A. Frerking, E. Brown, H. Grönqvist and S.M. Nilsen, "A Single Barrier Varactor Quintupler at 170 GHz," *IEEE Trans. Microwave Theory Tech.*, vol. 43, pp. 685-688, 1995.

[Simon 1993] A. Simon, A. Grüb, V. Krozer, K. Beilenhoff and H.L. Hartnagel, "Planar THz Schottky Diode Based on a Quasi Vertical Diode Structure," Fourth International Symposium on Space Terahertz Technology, Los Angeles, pp. 392-403, 1993.

[Stake 1996] J. Stake, L. Dillner and M. Ingvarson, "Fabrication and Characterisation of Heterostructure Barrier Varactor Diodes," Chalmers University of Technology, Department of Microwave Technology, Göteborg, Technical Report No. 29 (Revised) November 1996.

[Stake 1998] J. Stake, L. Dillner, S.H. Jones, C.M. Mann, J. Thornton, J.R. Jones, W.L. Bishop and E.L. Kollberg, "Effects of Self-Heating on Planar Heterostructure Barrier Varactor Diodes," *IEEE Trans. on Electron Devices*, vol. 45, pp. 2298-2303, 1998.

[Stake 1995] J. Stake and H. Grönqvist, "An On-Wafer Method for C-V Characterisation of Heterostructure Diodes," *Microwave Opt. Technol. Lett.*, vol. 9, pp. 63-66, 1995.

[Stake 1999a] J. Stake, S.H. Jones, L. Dillner and S. Hollung, "Heterostructure Barrier Varactor Design," *submitted to IEEE Trans. on Microwave Theory and Techniques*, 1999a.

[Stake 1997] J. Stake, S.H. Jones, J.R. Jones and L. Dillner, "Analysis of Carrier Transport in a Heterostructure Barrier Varactor Diode Tripler," 1997 International Semiconductor Device Research Symposium, Charlottesville, pp. 183-186, 1997.

[Stake 1999b] J. Stake, C.M. Mann, L. Dillner, S.H. Jones, S. Hollung, M. Ingvarson, H. Mohamed, B. Alderman and E.L. Kollberg, "Improved Diode Geometry for Planar Heterostructure Barrier Varactors," Tenth International Symposium on Space Terahertz Technology, Charlottesville, VA, 1999b.

[Sze 1981a] S.M. Sze, "Carrier Transport Phenomena: mobility," in *Physics of Semiconductor Devices*, 2nd ed. Singapore: JOHN WILEY & SONS, pp. 27-38, 1981a.

[Sze 1981b] S.M. Sze, *Physics of Semiconductor Devices*, 2nd ed. Singapore: JOHN WILEY & SONS, 1981b.

[Tang 1966] C.C.H. Tang, "An Exact Analysis of Varactor Frequency Multiplier," *IEEE Trans. Microwave Theory Tech.*, pp. 210-212, 1966.

[Thornton 1998] J. Thornton, C.M. Mann and P.d. Maagt, “Optimization of a 250-GHz Schottky Tripler Using Novel Fabrication and Design Techniques,” *IEEE Trans on Microwave Theory and Techniques*, vol. 46, pp. 1055-1061, 1998.

[Tuttle 1990] G. Tuttle, H. Kroemer and J.H. English, “Effects of interface layer sequencing on the transport properties of InAs/AlSb quantum wells: Evidence for antisite donors at the InAs/AlSb interface,” *J. Appl. Phys.*, vol. 67, pp. 3032-3037, 1990.

[Uhlir 1958] A. Uhlir, “The Potential of Semiconductor Diodes in High Frequency Communications,” *Proc. IRE*, vol. 46, pp. 1099-1115, 1958.

[Williams 1990] R. Williams, *Modern GaAs Processing Methods*, 2 ed: Artech House, 1990.

[Yngvesson 1991] S. Yngvesson, *Microwave Semiconductor Devices*: Kluwer Academic Publishers, 1991.